

Infra-red and Raman spectroscopy of free-base and zinc phthalocyanines isolated in matrices†

Ciaran Murray,^a Nadia Dozova,^a John G. McCaffrey,^{*a} Simon FitzGerald,^b Niloufar Shafizadeh^c and Claudine Crépin^c

Received 29th March 2010, Accepted 28th May 2010

DOI: 10.1039/c0cp00055h

The infrared absorption spectra of matrix-isolated zinc phthalocyanine (ZnPc) and free-base phthalocyanine (H₂Pc) have been recorded in the region from 400 to 4000 cm⁻¹ in solid N₂, Ar, Kr and Xe. Raman spectra have been recorded in doped KBr pellets. The isotopomers HDPc and D₂Pc have been synthesised in an attempt to resolve the conflicting assignments that currently exist in the literature for the N–H bending modes in H₂Pc spectra. A complete correlation between the vibrational modes of the three free-base isotopomers and ZnPc has been achieved. Comparison of the IR and Raman spectroscopic results, obtained with isotopic substitution and with predictions from large basis set *ab initio* calculations, allows identification of the in-plane (IP) and out-of-plane (OP) N–H bending modes. The largest IP isotope shift is observed in the IR at 1046 cm⁻¹ and at 1026 cm⁻¹ in Raman spectra while the largest effect in the OP bending modes is at 764 cm⁻¹. OP bending modes are too weak to be observed in the experimental Raman data. The antisymmetric N–H stretching mode is observed at ~3310 cm⁻¹ in low temperature solids slightly blue shifted from, but entirely consistent with the literature KBr data. With the exception of the N–H stretches, the recorded H/D isotope shifts in all the N–H vibrations are complex, with the IP bending modes exhibiting small $\nu_{\text{H}}/\nu_{\text{D}}$ ratios (the largest value is 1.089) while one of the observed OP modes has a ratio < 1. DFT results reveal that the small ratios arise in particular from strong coupling of the N–H IP bending modes with IP stretching modes of C–N bonds. The unexpected finding of a $\nu_{\text{H}}/\nu_{\text{D}}$ ratio smaller than one was analysed theoretically by examining the evolution of the frequencies of the free base by increasing the mass from H to D in a continuous manner. A consequence of this frequency increase in the heavier isotopomer is that the direction of the N–D OP bend is reversed from the N–H OP bend.

I. Introduction

Phthalocyanines (Pcs) are synthetic analogues of porphyrins in which nitrogen atoms in the aromatic polyene ring connect the four pyrrole groups instead of carbon. With an aryl group attached to each pyrrole the building block of the Pcs is, as shown in Fig. 1, the isoindole group. These very stable molecules are mostly used as dyes,¹ but have found several other applications as photoconductors,² as nonlinear optical materials³ and as photosensitisers in laser cancer therapy.⁴ Recently, with the use of only moderately intense laser excitation we observed amplified emission (AE) of zinc (ZnPc) and free-base phthalocyanine (H₂Pc) isolated in rare gas and nitrogen matrices.⁵ Because this effect was observed in thin samples (<100 μm) without the use of feedback optics, the Pcs are revealed as systems with extremely high optical gain. The mode exhibiting AE is a fluorescence transition from the vibrationless level of the first excited electronic state S₁ to a

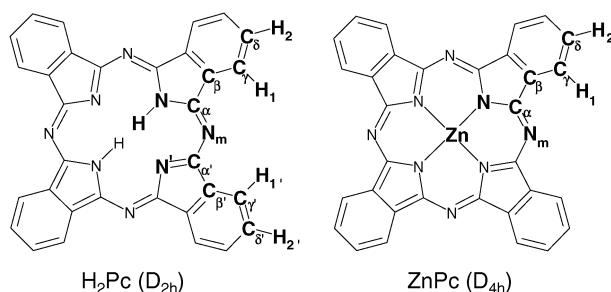


Fig. 1 The structures of free-base and zinc phthalocyanine determined by large basis [311 + +G(2d,2p)] set DFT geometry optimisation using the B3LYP functional. Both structures were found to be planar yielding molecular structures with D_{2h} and D_{4h} symmetries for H₂Pc and ZnPc respectively. The atom labelling used in these calculations is indicated while the geometric values determined are provided in Table S1 of the ESI.†

^a Department of Chemistry, National University of Ireland – Maynooth, Co. Kildare, Ireland. E-mail: john.mccaffrey@nuim.ie

^b Horiba Jobin Yvon Ltd, Stanmore, Middlesex, UK

^c Institut des Sciences Moléculaires d'Orsay, CNRS, Univ. Paris-Sud, F-91405 Orsay, France

† Electronic supplementary information (ESI) available: Details of the optimized geometries of ZnPc and H₂Pc are provided as are the predicted vibrational frequencies. See DOI: 10.1039/c0cp00055h

specific vibrationally excited level of the ground S₀ state. One purpose of the present work is to provide correct assignments for the ground state vibrational modes of H₂Pc and ZnPc. Indeed a complete vibrational analysis, involving comparison with narrow line experimental data, has not yet been made for these important molecules. In the present contribution we use matrix-IR absorption spectroscopy, isotope substitution,

Raman spectroscopy and high-level DFT calculations to conduct a vibrational analysis of zinc and free-base phthalocyanine.

An important aspect of the visible spectroscopy of H₂Pc which has not yet been resolved is the location of the origin of the S₂ (Q_Y) state. In the gas phase the vibronic structure present in the excitation spectra is so complex in the onset region of the Q_Y state that the band origin of this state has not been identified.^{6,7} Extreme spectral congestion arises in the region where the $\nu = 0$ level of the Q_Y state overlaps the vibrationally excited levels of the Q_X (S₁) state rendering visual identification of the origin impossible. Due to the similar energy splitting between the Q_X and Q_Y states in matrix spectra and the assumed transition energy of the N–H in-plane bending vibration, this mode is considered to be important in the coupling between the two electronic states.⁸ Since the vibrational modes in the ground S₀ state and the first excited Q (S₁) state are very similar,^{9,10} vibrational assignments in the ground state are essential for analysing the complex vibronic structure in the electronic excitation spectra. As a precursor to an analysis of the excitation and emission spectra, which will be presented in a forthcoming article,¹⁰ an analysis of the fundamental vibrational modes is required and undertaken herein.

While several infrared studies have been presented for H₂Pc^{11,12} and ZnPc¹³ in KBr discs and in Nujol, no reports currently exist for the low temperature IR spectra of these molecules. Despite the numerous infrared studies of H₂Pc which have been published, the assignments of several vibrational modes remain uncertain, especially in the case of the N–H In-Plane Bending (NH-IPB) mode. This vibrational mode has been assigned to bands at 1006 cm⁻¹ and 1539 cm⁻¹ in experimental work.^{11,12} Theoretical calculations of the infrared and Raman active vibrations for H₂Pc¹⁴ and ZnPc¹⁵ have also been published. The most detailed vibrational analysis to-date of H₂Pc has been done by Zhang *et al.*,¹⁴ who conducted a DFT calculation utilising the B3LYP functional and a 6-31G* basis set.

Investigation of the infrared spectra of H₂Pc and its isotopomers using the matrix-isolation technique should allow conclusive identification of the NH-IPB mode. The IR spectra obtained under these conditions are those of isolated molecules and are largely free of bands arising from interactions present in phthalocyanine aggregates. Moreover, because of the low temperatures used, thermal population of the lowest frequency modes of the Pcs, which are known to exist, is almost completely eliminated. An illustration of the improvement in the data obtained from matrix samples is provided by the comparison shown in Fig. 2 for spectra recorded for H₂Pc in solid Ar at 14 K and in KBr discs at room temperature. It is immediately evident in this figure that the matrix bands are narrower and much better resolved than those present in the KBr spectra. A similar comparison of the ZnPc spectra is presented in Fig. S1 of the ESI.†

In the present paper we describe, for the first time, a study of the matrix infrared absorption spectra of H₂Pc and its isotopomers HD₂Pc and D₂Pc isolated in rare gas and inert molecular solids. ZnPc, which does not contain the central N–H bonds of interest, was also studied under the same conditions for the purposes of comparison. In addition, Raman spectra of ZnPc, H₂Pc and D₂Pc were recorded in

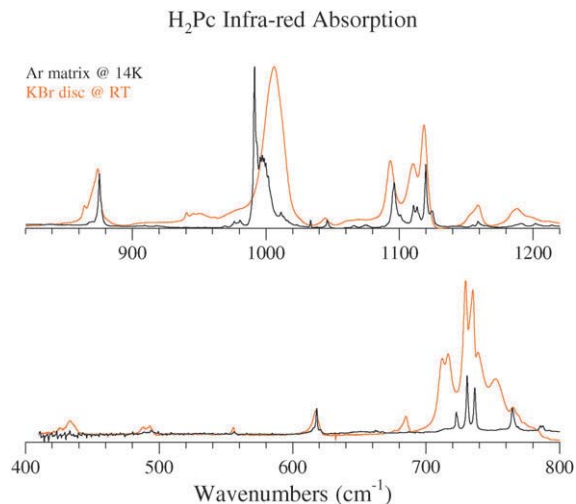


Fig. 2 A comparison of the infrared absorption spectra recorded for H₂Pc trapped in an Ar matrix at 14 K and in a KBr pellet at room temperature. Major differences in the spectra are evident in the 740 and 1000 cm⁻¹ regions, both of which have been attributed to the N–H bending modes in the literature.

KBr discs. Large basis set DFT calculations were performed on the four aforementioned molecules in order to assign the observed vibrational modes. These calculations are essential for assignments of the vibrational modes present in both Raman scattering and visible fluorescence spectra recorded previously by our group⁵ with Q-band excitation of matrix-isolated Pcs.

After presenting an outline in Part II of the experimental and computational methods employed, a brief overview of the results obtained is provided in Part III. Part IV is devoted to a discussion of both the experimental and computational data obtained for ZnPc and H₂Pc and the isotopomers HD₂Pc and D₂Pc. This section is divided into three parts, dealing with (A) IR spectra, (B) Raman spectra and (C) specific isotopic effects. The main conclusions are summarized in Part V.

II. Methods

A Experimental

ZnPc and H₂Pc were purchased from Sigma Aldrich and Fluka, respectively, and used without further purification. Matrix samples were prepared by heating the phthalocyanines to around 350 °C and using the flowing host gas to entrain the Pc vapour for deposition on a KBr window at cryogenic temperatures. The cryogenic set-up has been described previously.¹⁶ The oven⁵ used consisted of a solid stainless steel cylinder in which a hollow screw, containing either ZnPc or H₂Pc, was fitted. The top of this screw was positioned to emerge at right angles to a 2 mm opening passing the length of the cylinder. This opening was connected by a Swagelok compression seal to a $\frac{1}{4}$ " gas inlet line. Resistive heating of the cylinder was used to reach vaporisation temperatures. Large gas flows (40 mmol h⁻¹) were required to achieve isolation of the Pc as a monomer.

Infrared absorption spectra in solid N₂, Ar, Kr and Xe were recorded on a Bruker IFS/66s spectrometer in the Low Temperature Spectroscopy (LTS) group at NUI-Maynooth

at a resolution of 0.5 cm^{-1} . Two IR detectors were used to record spectra, namely a liquid- N_2 cooled MCT was used in the region down to 800 cm^{-1} while a room temperature DTGS was used for the lower frequency range down to 400 cm^{-1} . The spectrometer was purged with dry air in order to reduce contributions from water vapour lines in the spectral regions of interest. The samples were deposited on a KBr window at 20–25 K for Ar and N_2 matrices. Slightly higher temperatures of 25–27 K were used in the heavy rare gas matrices Kr and Xe, in order to avoid the formation of highly scattering samples. All spectra were recorded at 13 K. The spectra of ZnPc and H_2Pc were not sensitive to the temperature at which they were recorded and moderate annealing to 25, 25, 30 and 35 K in N_2 , Ar, Kr or Xe matrices, respectively, had no effect on the line shapes and positions. The duration of a typical deposition was 1 h. These long deposition times were required to achieve acceptable absorption strengths and are at least twice as long as used for the samples used in visible spectroscopic studies.

Raman spectroscopy of ZnPc and H_2Pc in KBr discs was performed using a LabRAM HR confocal Raman microscope (HORIBA Scientific). Excitation was from a narrowband ($<1\text{ MHz}$) diode-pumped, solid state 532 nm Nd:YAG laser, whose power was typically adjusted to 8 mW at the sample. The Pcs exhibit an absorption dip at this excitation wavelength so the resulting Raman scatter is largely free of fluorescence and resonance Raman contributions. In addition self-absorption of the weaker, low-frequency Raman modes is minimised with the use of the 532 nm laser. Spectra were also recorded with 633 nm excitation but, because of the strong fluorescence background, are not presented herein. A Peltier ($-70\text{ }^\circ\text{C}$) cooled 1024×256 pixel CCD detector, with an open electrode format, was used for detection. Using a visible-optimised 600 gr mm^{-1} diffraction grating, the 800 mm focal length spectrometer provides a spectral resolution of 3 cm^{-1} . Backscattered light was collected through the microscope optics, using a Leica ($\times 50$) long-working-distance objective (NA = 0.55). Several point measurements were made on each KBr disc to ensure sample homogeneity.

Deuterated free-base phthalocyanine (D_2Pc) was prepared using a procedure similar to that described by Fitch *et al.*,¹⁷ where the two inner hydrogen atoms were exchanged with a deuterated acid. In the following procedures, one D_2Pc sample was prepared using deuterated trichloroacetic acid (TCA- d_1) and another sample with deuterated trifluoroacetic acid (TFA- d_1). TCA- d_1 was prepared by adding 12 ml of D_2O (Apollo Scientific, 99.9% D-atom purity) to 48.6 g trichloroacetic acid (Sigma Aldrich). The solution was heated to approximately $70\text{ }^\circ\text{C}$ and the water was removed by vacuum distillation. The process was repeated 5 times to maximise deuteration. Deuterated phthalocyanine was prepared by adding 0.5 g of normal free-base phthalocyanine to the deuterated TCA prepared above. This mixture was equilibrated under Ar at $80\text{ }^\circ\text{C}$ with continuous stirring for 3 h. The D_2Pc was precipitated by addition of 30 ml of D_2O . The precipitate was filtered, washed 5 times with hot D_2O and dried in an oven at $110\text{ }^\circ\text{C}$. A second sample of D_2Pc was prepared using 99.5% D trifluoroacetic acid- d_1 purchased from Sigma Aldrich. Under Ar, 0.5 g of normal free-base phthalocyanine was

added to 25 g of TFA- d_1 and was refluxed for 3 h. As with the preparation using TCA- d_1 , the D_2Pc was precipitated with 30 ml D_2O , filtered, washed with hot D_2O and dried in an oven at $110\text{ }^\circ\text{C}$.

In both syntheses, mixtures of H_2Pc , HDPC and D_2Pc resulted. The compositions of mixture 1 (obtained from synthesis 1) and mixture 2 (obtained from synthesis 2) were slightly different. By assuming that the relative intensities of the N–H stretching modes in H_2Pc and in HDPC is 2/1 and of the N–D modes in HDPC and in D_2Pc is equal to 1/2, the relative amounts of the three species were determined for the two mixtures with the following results. For mixture 1: $\text{H}_2\text{Pc}/\text{HDPC}/\text{D}_2\text{Pc} = 13\%/40\%/47\%$ and for mixture 2: $15\%/46\%/39\%$. A third mixture was prepared for Raman experiments in KBr pellets. Its composition, determined from N–H and N–D stretching mode intensities, was found to be $12\%/36\%/52\%$ for $\text{H}_2\text{Pc}/\text{HDPC}/\text{D}_2\text{Pc}$.

B Computational

All calculations were performed with the Gaussian 03 quantum chemistry package¹⁸ using Density Functional Theory (DFT). The B3LYP^{19–21} functional was used with the 6-311++G(2d,2p) basis set by Pople *et al.*²² for both geometry optimisation and harmonic frequency calculation. To the best of our knowledge, this is the largest basis set used to date on the H_2Pc and ZnPc systems. The calculations were run at NUI-Maynooth on a Linux workstation with two AMD “Barcelona” 64-bit quad-core processors running at 2.0 GHz. To allow comparison with experimental bands, we choose to apply a uniform scaling factor²³ in the spectral region below 2000 cm^{-1} . Accordingly, all the computed frequencies in this range are uniformly multiplied by 0.98, which was found to give the best agreement when compared with the experimental results. The scaling factors used for the higher frequency CH and NH stretching vibrations are 0.96 and 0.931 respectively.

The Gaussian 03 computed scattering activity, S_i ($\text{\AA}^4\text{ amu}^{-1}$) of a normal mode i , has been transformed into Raman intensity, I_i ($\text{m}^2\text{ sr}^{-1}$), for comparison with recorded Raman data. This is achieved with the expression,

$$I_i = \frac{C(\nu_0 - \nu_i)^4 S_i}{\nu_i B_i} \quad (1)$$

presented by Michalska and Wysokinski.²⁴ In eqn (1) ν_0 is the energy of the incident 532 nm laser light ($18\,797\text{ cm}^{-1}$) and ν_i is that of a normal mode i . The C term is a constant made up of a geometry factor and the physical constants h , k and c Planck’s, Boltzmann’s constants and the speed of light respectively. B_i is the Boltzmann distribution of population amongst the normal modes and its dependence on temperature T is given by

$$B_i = 1 - \exp\left(\frac{-h\nu_i c}{kT}\right) \quad (2)$$

This term may be ignored for experiments conducted at very low temperatures or for modes with frequencies above $\sim 500\text{ cm}^{-1}$ when its value approaches 1. However, as the Raman spectra presented herein were recorded at room temperature and the Pcs have several modes below 300 cm^{-1} , inclusion of

the B_1 correction has a significant effect on the intensities of the lower frequency modes in the computed spectra.

III. Results

A Experimental

1 ZnPc. An infrared absorption spectrum recorded for ZnPc isolated in a N_2 matrix is shown in the upper panel of Fig. 3. The most intense infrared active bands of this molecule are situated between 400 and 1650 cm^{-1} . Other less intense bands, arising from C–H stretching modes are located, as

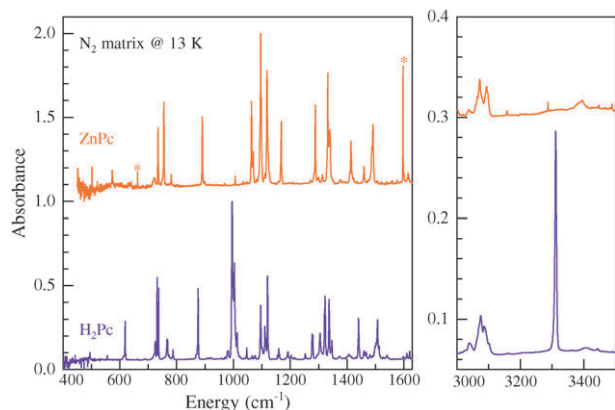


Fig. 3 Infrared spectra of ZnPc and H_2Pc molecules isolated in a N_2 matrix at 13 K in the two spectral regions with the strongest absorptions. The asterisks (*) denote small amounts of the matrix-isolated impurities carbon dioxide and water.

Table 1 Infrared frequencies (in cm^{-1}) observed for ZnPc trapped in different solids. The symmetries provided were obtained from DFT calculations. The corresponding theoretical frequencies have been scaled by a factor of 0.98 below 2000 cm^{-1} , while a value of 0.96 has been used for the C–H modes in the vicinity of 3000 cm^{-1} . The symmetry labels given for the molecular vibrations of ZnPc utilise the D_{4h} group. The experimental values shown in bold are the most intense bands. Values indicated by an asterisk are possible combination bands, while those indicated by “sh” are unresolved shoulders on more intense bands

KBr	Ar	Kr	Xe	N_2	DFT (scaled)	DFT (unscaled)	Sym.
435	—	—	430.0	—	437.3	446.2	A_{2u}
499	502.2	—	501.2	502.0	501.4	511.4	E_u
571	573.4	573.8	572.0	573.4	574.1	585.8	E_u
635	637.3	—	640.4	640.7	639.8	652.8	E_u
727	732.7	731.5	730.8	733.9	734.0	749.0	A_{2u}
752	754.4	754.4	754.0	754.7	752.6	768.0	E_u
782	778.8	778.2	777.7	780.8	781.1	797.0	A_{2u}
887	890.1	889.6	889.4	890.2	887.9	906.0	E_u
1004	1004.7	1004.5	1003.7	1005.5	1009.4	1030.0	E_u
1060	1063.1	1062.4	1061.4	1063.6	1062.8	1084.5	E_u
—	1069.3	1068.4	1068.6	1070.2	—	—	—
1088	1094.8	1094.5	1093.6	1095.9	1089.0	1111.1	E_u
1116	1117.4	1116.8	1114.5	1117.8	1115.5	1138.2	E_u
1164	1167.7	1167.3	1165.7	1168.2	1166.2	1190.0	E_u
1285	1287.1	1287.1	1285.8	1288.1	1294.0	1320.4	E_u
—	1296.0	1295.0	1292.1	1297.8	—	—	—
—	1310.7	1307.8	1306.6	1313.5	1316.9	1343.8	E_u
1331	1331.8	1331.5	1331.8	1332.2	1332.4	1359.6	E_u
—	1338.0	1337.6	1336.8	1339.4	—	—	—
1409	1412.2	1411.7	1410.5	1413.5	1407.9	1436.6	E_u
1454	1459.3	1458.1	1458.4	1459.7	1461.2	1491.0	E_u
1482	1491.0	1490.4	1488.9	1491.0	1481.4	1511.6	E_u
1607	—	—	1613.9	1615.1	1608.5	1641.3	E_u
3024*	3035.1*	3034.8*	3031.1*	3038.3*	—	—	—
3047	3061.5 ^{sh}	3059.1 ^{sh}	3054.0 ^{sh}	3064.0 ^{sh}	3061.3	3174.0	E_u
3055	3069.2	3067.6	3061.1	3072.3	3074.4	3187.6	E_u
3077	3093.8	3092.1	3086.7	3093.5	3091.0	3204.8	E_u

shown in the panel on the right, around 3100 cm^{-1} . Weak bands observed between 1650 and 3000 cm^{-1} are expected to be combination modes and were not investigated. The most intense vibrational bands of ZnPc in the mid-IR are situated at 1095.9, 1117.8 and 1332.2 cm^{-1} in N_2 matrices. Weaker bands in the C–H stretching mode region are, as shown in the right hand panel, situated at 3038.3, 3072.3 and 3093.5 cm^{-1} . The spectra of ZnPc in other matrices (Ar, Kr and Xe) are similar to the spectrum shown for N_2 in Fig. 3, but the bands shift slightly to lower energies.

The observed vibrational bands are in good agreement with the KBr disc IR spectrum published by Tackley *et al.*,¹³ although as shown in Fig. S1 (ESI[†]), the bands in cryogenic matrices are much narrower and better resolved. The frequencies of the observed fundamental modes in all matrices studied are given in Table 1 along with KBr data recorded in the present work. Very small shifts of vibrational frequencies are noticeable from one host gas to another but these are all shifted to the blue of the KBr bands. In cryogenic matrices, the bands are quite narrow, except in the CH stretch region. The structure in this region may be due to site effects, since the C–H bonds of the aryl group are located on the outer part of the molecule. As a result, these stretching modes are very sensitive to the trapping environment as revealed by the pronounced ($> 20 cm^{-1}$) KBr–matrix shift.

Raman spectra of ZnPc were recorded only in KBr pellets at room temperature. The 100–1700 cm^{-1} range is shown in the upper panel of Fig. 4. The most intense bands are situated at 676.5, 1338.3 and 1506.8 cm^{-1} . As expected, the results we obtained with 532 nm excitation compare well with the

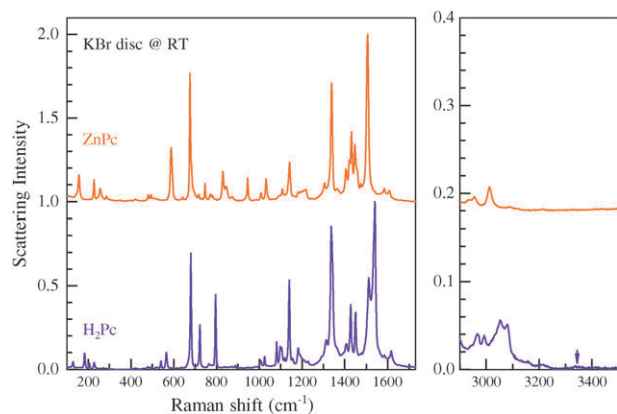


Fig. 4 Raman spectra of ZnPc and H₂Pc in KBr pellets recorded at room temperature with 532 nm excitation. Conspicuous in the high frequency spectral region is the absence of a strong symmetric N–H stretch which is quite pronounced in the corresponding IR spectrum of H₂Pc. Its possible location, obtained with DFT prediction, is indicated by the arrow.

spectrum recorded by Tackley *et al.*¹⁵ with an excitation wavelength of 514 nm. Beyond 1700 cm⁻¹, the Raman spectrum exhibits several bands, consisting mostly of overtones or combination bands, so that, the C–H stretching modes are difficult to identify clearly. On the other hand, our results reveal only four very low frequency (below 400 cm⁻¹) modes. The frequencies of the recorded Raman bands are collected in Table 2.

2 H₂Pc. The IR spectrum of H₂Pc in N₂ is shown in the lower panel of Fig. 3. The main difference with the spectrum of ZnPc is the appearance of two new intense bands—a triplet centred around 1000 cm⁻¹ and a sharp singlet at 3311.5 cm⁻¹. These bands have been attributed in the infra-red spectra of KBr discs¹² to the N–H deformation and N–H stretching modes respectively. The latter assignment is entirely appropriate, the former will be examined in detail in the present paper. Spectra recorded in other matrices (Ar, Kr and Xe) are similar to the one shown in Fig. 3 for N₂ but are also shifted to lower energies. As in the case of ZnPc, all the bands are narrow, except those corresponding to CH stretching modes between 3000 and 3100 cm⁻¹. The frequencies of the observed modes of H₂Pc in all matrices studied are collected in Table 3. Spectral shifts from one matrix host to another are very small, but as previously found with ZnPc, the shifts are larger between KBr and the inert gas hosts. The most pronounced KBr–matrix shift is found for the N–H stretching mode. The IR signatures of ZnPc and H₂Pc can be compared in Fig. 3, illustrating the differences between the entries in Tables 1 and 3 for these molecules.

The infrared absorption spectrum of H₂Pc in KBr discs has been published previously by Shurvell and Pinzuti.¹¹ As found in ZnPc, the H₂Pc bands in KBr are red-shifted and broadened compared to the matrix bands because of the interaction between dopant molecules in KBr. This effect is clearly evident in Fig. 2 which presents a comparison of the spectra recorded in solid Ar and in KBr. However, in contrast to the ZnPc system (Fig. S1, ESI†), several significant differences

exist between the KBr and matrix spectra of H₂Pc. The most significant differences are evident in the 740 and 1000 cm⁻¹ regions, which have been the subject of much debate and confusion. Several bands present in KBr (685, 712.1 and 716.5 cm⁻¹) are absent in the matrix spectra. The fact that they are absent or observed with a drastic reduction in intensity (compared to the bands around 730 and 736 cm⁻¹) in the matrix spectra indicates that these bands are due to H₂Pc aggregates. The strongest band in KBr at 1006.5 cm⁻¹ is much narrower and located at a lower frequency (995 cm⁻¹) in the N₂ matrix. All other modes in inert host matrices are observed at higher energy than in KBr.

The Raman spectrum of H₂Pc in KBr discs, recorded under the same conditions as ZnPc in KBr, is shown in the lower panel of Fig. 4 while the corresponding vibrational frequencies are reported in Table 2. The similarities between H₂Pc and ZnPc Raman spectra are striking, and much more extensive than between the corresponding IR spectra shown in Fig. 3. This behaviour would immediately suggest that the N–H modes of free-base phthalocyanine are only weakly Raman active.

3 Deuteration effects. The two syntheses of D₂Pc used in matrix-IR experiments yielded mixtures of H₂Pc, HDPc and D₂Pc with, as shown by the lower traces in Fig. 5, slightly different compositions for two spectra recorded in Ar. The plot on the right shows the N–H stretching region. The less intense band at 3310.0 cm⁻¹ is the antisymmetric stretching of H₂Pc, which was already observed in pure H₂Pc samples and is shown for comparison by the black trace in Fig. 5 (bottom). The more intense band is the N–H stretching of HDPc at 3337.1 cm⁻¹. The left panel in Fig. 5 shows the region of the N–D stretching. The highest energy feature at 2538.6 cm⁻¹ is a combination band already present in the spectrum of pure H₂Pc shown by the black trace. The absorption at 2480.5 cm⁻¹ is more intense in mixture 1 and since this sample contains most D₂Pc, this band is assigned to the N–D antisymmetric stretching mode of the fully deuterated molecule.

This assignment is supported by data extracted from the difference spectra. Difference spectra containing only HDPc or D₂Pc were obtained with the following procedure. First: the spectrum of pure H₂Pc is multiplied by a coefficient and subtracted from those of mixtures 1 and 2, so in the difference spectra the intensity of the pure N–H stretching mode in H₂Pc (in argon the band at 3310 cm⁻¹) is equal to 0. Two spectra, containing only HDPc and D₂Pc: mixtures 1' and 2', are thereby obtained. Second: the spectrum of 1' is multiplied by a coefficient and subtracted from spectrum 2' so the intensity of the N–D stretching mode band of D₂Pc (at 2480.5 cm⁻¹ in Ar) is equal to 0. This difference spectrum is now that of pure HDPc. Third: the spectrum of 2' is multiplied by a coefficient and subtracted from spectrum 1', so the intensity of the band of HDPc at 3337.1 cm⁻¹ in Ar (N–H stretching mode) is equal to 0. This difference spectrum shows only D₂Pc bands.

The difference spectra generated for HDPc and D₂Pc isolated in an Ar matrix are presented in the upper panels of Fig. 5 in the N–D (left panel) and N–H (right panel) stretching regions. Two unaccounted bands are located at 2501.4 and 2523.3 cm⁻¹ in the raw spectra of both the mixtures but with

Table 2 Vibrational frequencies (in cm^{-1}) measured in KBr pellets for the Raman active modes of D_2Pc , H_2Pc and ZnPc . The DFT results are provided both unscaled and scaled by a factor of 0.98. Symmetry assignments for the molecular vibrations were obtained from the DFT results. The strongest bands observed in the recorded spectra are shown in bold; relative intensities in brackets

D_2Pc Obs.	H_2Pc			Sym.	ZnPc			Sym.
	Obs.	Calc. scaled	Calc. unscaled		Obs.	Calc. scaled	Calc. unscaled	
128.7 (w)	129.9 (w)	130.2 (0.0017)	132.9	A_g	157.4 (m)	154.5 (0.001)	157.6	B_{1g}
183.7 (m)	182.9 (m)	177.6 (0.0015)	181.2	B_{1g}	228.3 (m)	227.2 (0.0016)	231.8	B_{2g}
206.0 (w)	204.7 (w)	207.7 (0.0000)	211.9	B_{1g}				
228.3 (w)	228.3 (w)	225.4 (0.004)	229.7	A_g	257.2 (w)	253.2 (0.003)	258.4	A_{1g}
					286.0 (w)	282.6 (0.0000)	288.4	E_g
479.4 (w)	479.9 (w)	477.9 (0.007)	487.6	B_{1g}	479.9 (w)	479.9 (0.0060)	489.7	B_{2g}
					494.0 (w)	498.5 (0.0000)	508.7	E_g
540.4 (w)	541.3 (w)	540.3 (0.002)	551.3	A_g				
565.6 (m)	565.7 (m)	566.0 (0.002)	577.5	A_g	588.3 (s)	588.1 (0.0060)	600.1	A_{1g}
					642.0 (w)	645.9 (0.0000)	659.1	E_g
680.0 (s)	679.9 (s)	676.6 (0.02)	690.4	A_g	676.5 (vs)	676.1 (0.0160)	689.9	A_{1g}
					717.2 (w)	724.3 (0.0000)	739.1	E_g
720.2 (m)	722.8 (m)	728.6 (0.06)	743.5	A_g	746.8 (w)	749.5 (0.050)	764.8	B_{1g}
764.7 (vw)	764.7 (vw)	763.7 (0.001)	779.3	A_g	772.3 (vw)	772.3 (0.020)	788.7	B_{1g}
					782.0 (vw)	792.8 (0.0002)	809	E_g
794.5 (s)	796.1 (s)	794.5 (0.01)	810.7	A_g	830.0 (m)	834.5 (0.0080)	851.6	A_{1g}
					845.0 (w)			
					873.0 (w)	879.8 (0.0000)	897.8	E_g
888.1 (w)	888.9 (w)	889.3 (0.0000)	907.4	B_{1g}				
1006.9 (w)	1007.3 (w)	1008.4 (0.012)	1029.0	A_g	1008.9 (w)	1009.8 (0.026)	1030.4	A_{1g}
986.1 (w)	1026.3 (w)	1028.7 (0.012)	1049.7	B_{1g}	1032.0 (m)	1035.5 (0.006)	1056.6	B_{2g}
1026.3 (w)								
1044.1 (m)	1081.4 (m)	1084.8 (0.002)	1107.0	B_{1g}	945.8 (m)	944.3 (0.0020)	963.6	B_{2g}
1082.7 (m)								
1097.6 (m)	1099.1 (m)	1099 (0.0000)	1121.7	B_{1g}				
1105.0 (m)	1104.4 (m)	1109.9 (0.02)	1132.5	B_{1g}	1107.6 (w)	1109.3 (0.019)	1131.9	B_{2g}
1116.9 (vw)	1117.4 (w)	1116.0 (0.05)	1138.3	A_g				
1139.2 (s)	1140.3 (s)	1140.7 (0.13)	1164.0	A_g	1141.9 (m)	1141.0 (0.144)	1164.3	B_{1g}
1155.6 (w)	1154.9 (vw)	1161.3 (0.18)	1185.2	A_g				
1183.8 (vw)	1180.9 (w)	1179.9 (0.06)	1211.4	A_g	1182.5 (w)	1178.1 (0.066)	1202.1	B_{1g}
	1190.0 (vw)	1191.1 (0.006)	1223.6	B_{1g}	1197.1 (w)			
1217.9 (w)	1227.8 (w)	1233.5 (0.14)	1258.7	B_{1g}	1210.0 (w)	1207.4 (0.037)	1232.0	B_{2g}
1290.8 (sh)	1293.7 (sh)	1300.4 (0.30)	1327.0	A_g	1218.1 (w)	1296.5 (0.35)	1323.0	B_{1g}
1313.1 (w)	1312.8 (w)	1312.5 (0.01)	1339.3	B_{1g}	1304.9 (w)	1304.8 (0.0230)	1331.4	B_{2g}
1335.4 (vs)	1336.7 (vs)	1333.7 (0.13)	1360.9	A_g	1338.3 (vs)	1336.5 (0.107)	1363.8	A_{1g}
1344.3 (vs)		1345.8 (0.14)	1373.3	A_g		1341.5 (0.088)	1368.9	B_{1g}
1402.2 (m)	1406.5 (w)	1393.9 (0.025)	1422.4	A_g	1404.9 (m)	1393.0 (0.030)	1421.4	A_{1g}
1427.5 (s)	1426.9 (m)	1430.8 (0.05)	1459.0	B_{1g}	1431.7 (m)	1427.9 (0.024)	1457.0	B_{2g}
		1431.6 (0.148)	1460.9					
1449.8 (m)	1450.5 (m)	1452.0 (0.09)	1481.6	A_g	1447.4 (m)	1449.1 (0.101)	1478.7	B_{1g}
					1474.0 (w)	1479.4 (0.011)	1509.6	B_{2g}
1518.1 (s)	1511.5 (s)	1510.3 (0.09)	1541.1	A_g				
1540.4 (vs)	1539.5 (vs)	1551.2 (1.0)	1582.9	A_g	1506.8 (vs)	1526.0 (1.0)	1557.2	B_{1g}
1583.5 (w)	1584.4 (w)	1579.1 (0.006)	1611.4	A_g	1584.4 (w)	1582.4 (0.004)	1614.7	B_{1g}
1616.2 (w)	1616.8 (w)	1613.9 (0.004)	1646.8	B_{1g}	1607.6 (w)	1609.6 (0.0016)	1642.5	B_{2g}

the help of difference spectra, the former can be assigned to the N–D stretching in HDPc . In conclusion, the N–H and N–D stretching modes of HDPc are at 3337.1 and 2501.4 cm^{-1} respectively.

The overlap between the bands of the three isotopomers in the 400 to 1600 cm^{-1} region does not allow us to use the raw mixture spectra to identify the lower frequency modes for each species. This problem can be resolved if “difference” spectra are used instead. The signal-to-noise ratio of these spectra is lower than in the original mixture spectra and as a result, this method can only be used to analyse the most intense IR bands.

Fig. 6 and 7 show the difference spectra extracted for HDPc and D_2Pc in the 700–800, the 900–1150 and the 1150–1300 cm^{-1} regions together with the pure H_2Pc spectrum. Other than the N–H(D) stretching regions, these are the spectral ranges where the largest shifts were observed between the spectra of the

three isotopomers. All the other bands are only slightly shifted ($< 2 \text{ cm}^{-1}$) upon H/D substitution. As shown in the left panel of Fig. 6, the band of H_2Pc at 764.8 cm^{-1} in Ar appears to shift to 742.5 cm^{-1} in HDPc . No new bands are observed for D_2Pc in the lower energy part of the spectrum shown. On the other hand, the strong 728 cm^{-1} band of D_2Pc exhibits, as shown in Fig. 6, a structure whose resolution depends strongly on the matrix host. The spectra recorded in N_2 matrices (centre panel) are the best resolved and reveal the presence of two bands for D_2Pc at 728.0 and 731.4 cm^{-1} instead of one broad, but intense band in Ar and Kr. Assuming a pair of lines is also present in the Ar and Kr data—a reasonable assumption given their widths and indications of unresolved structure on both—then in N_2 the three bands of H_2Pc at 724.7, 730.9 and 736.4 cm^{-1} are located at 722.1, 728.0 and 731.4 cm^{-1} in D_2Pc . This proposal will be examined further in

Table 3 Infrared frequencies (in cm^{-1}) observed for H_2Pc trapped in different solids. The DFT results shown have been scaled with the same factors as used in Table 1. The symmetry labels given for the vibrations utilise the D_{2h} point group, with the z -axis perpendicular to the molecular plane. Some of the weakest unassigned bands may arise from site splitting or H_2Pc aggregates. Asterisks and “sh” have the same meaning as in Table 1. The strongest bands observed are shown in bold

KBr	Ar	Kr	Xe	N_2	DFT (scaled)	DFT (unscaled)	Sym.
493	494.3	494.6	493.4	494.4	492.5	502.6	B_{3u}
556	556.6	555.8	556.0	556.2	556.0	567.4	B_{3u}
618	618.2	617.9	617.5	618.4	619.6	632.3	B_{3u}
	722.7	722.0	721.2	724.7	725.7	740.5	B_{1u}
730	731.0	730.6	730.5	730.9	731.5	746.5	B_{3u}
735	736.6	736.3	735.9	736.4	735.8	750.8	B_{2u}
765	764.8	764.6	762.6	766.9	762.8	778.4	B_{1u}
—	785.6	784.7	783.6	787.4	783.1	799.1	B_{3u}
874	875.4	874.8	875.3	875.7	874.0	891.8	B_{3u}
—	980.9	980.4	976.0	980.8	—	—	—
1007	991.5	995.7	994.6	995.0	1016.5	1037.2	B_{3u}
—	997.6	1001	1001.0	1003.0	—	—	—
	1011.3	1011.1	1010.4	1012.7	—	—	—
1045	1046.2s	1045.4	1045.7	1047.1	1047.0	1068.4	B_{2u}
	1065.4	1064.8	1064.5	1065.9	1064.3	1086.9	B_{3u}
	1075.7	1072.9	1070.2	1074.9	—	—	—
1094	1096.1	1095.0	1094.2	1096.0	1086.9	1109.0	B_{2u}
1110	1110.7	1110.5	1101.3	1112.4	1109.3	1131.9	B_{3u}
1118	1120.0	1119.2	1118.6	1120.6	1116.8	1139.6	B_{2u}
	—	1154.8	1152.5	1155.3	1157.8	1181.4	B_{2u}
1160	1158.9	1158.1	1157.6	1159.7	1162.4	1186.1	B_{3u}
1189	1191.1	1190.5	1188.7	1192.2	1190.3	1214.6	B_{2u}
—	1201.8	1200.0	1197.9	1202.5	—	—	—
	1251.6	1252.0	1251.5	1252.7	1260.7	1286.4	B_{2u}
1277	1276.2	1277.9	1277.3	1277.3	1286.3	1312.6	B_{3u}
	1279.0	—	—	1280.2	—	—	—
1303	1302.2	1301.2	1300.0	1305.3	1307.4	1334.1	B_{2u}
	1309.0	1307.5	1307.4	—	—	—	—
1321	1322.2	1322.2	1321.5	1323.2	1313.1	1339.9	B_{2u}
1335	1336.6	1336.1	1336.5	1336.4	1331.6	1358.8	B_{3u}
1343 ^{sh}	1346.5	1345.9	1345.5	1346.7	1343.1	1370.6	B_{2u}
1438	1440.8	1439.9	1438.9	1441.1	1444.0	1473.5	B_{2u}
—	1459.5	1459.5	1460.0	1459.4	—	—	—
1459	1466.5	1464.9	1461.9	1466.8	1460.8	1490.7	B_{3u}
—	1496.3	—	—	1494.9	—	—	—
—	1498.8	1498.4	1497.6	1498.4	1499.4	1530.0	B_{2u}
	1501.2	—	—	1501.6	—	—	—
1503	1506.1	1505.2	1504.3	1507.3	1500.9	1531.5	B_{3u}
—	1513.1	1512.0	—	1513.1	—	—	—
	—	1538.7	1537.9	1540.8	1536.5	1567.9	B_{2u}
1609	1607.8	1610.3	1608.8	1610.7	1606.3	1639.1	B_{3u}
	1623.5	1620.1	1618.7	1621.1	1613.8	1646.8	B_{2u}
3049*	3039.6*	3035.2*	3034.6*	3041.0*	—	—	—
—	3063.4 ^{sh}	3057.9 ^{sh}	—	—	3058.6	3172.8	B_{3u}
	—	—	—	—	3063.8	3176.6	B_{2u}
—	3072.8	3070.4	3066.0	3075.6	3073.4	3186.5	B_{2u}
	—	—	—	—	3076.8	3190.1	B_{3u}
3075	3086.1	3082.3	3079.5	3087.2	3089.9	3203.6	B_{2u}
	—	—	—	—	3093.0	3207.8	B_{3u}
3289	3310.0	3308.1	3309.2	3311.5	3307.3	3556.3	B_{3u}

conjunction with the discussion of the DFT predictions of isotopic shifts.

The left panel of Fig. 7 shows the spectral range from 900 to 1150 cm^{-1} in solid Ar in which it is immediately evident that this region is dominated by the strong 1000 cm^{-1} band. However, a pronounced shift is not exhibited upon isotopic substitution by the most intense band located at 991.5 cm^{-1} . Concentration studies reveal that the 1000 cm^{-1} band changes extensively on the high energy side indicating that the blue region is where aggregates of the Pcs absorb. Thus in the D_2Pc spectrum presented on the top in Fig. 7, the most intense feature is shifted towards the blue but this effect is arising as a result of an increased amount of aggregates and is not an

isotope effect. As indicated by the asterisks in Fig. 7, the location of the monomer band is only very slightly isotope dependent. The observed positions for the monomer bands of H_2Pc , HDPc and D_2Pc in solid Ar are 991.5 , 990.4 and 989.3 cm^{-1} respectively.

In contrast to the dominant band, several of the weaker bands in this region do show pronounced H/D isotope dependence. As indicated by the arrow on the extreme left in Fig. 7, D_2Pc has a strong band at 964.1 cm^{-1} which is not present in the two lighter isotopomers. HDPc does exhibit a new band at 977.8 cm^{-1} (red downward arrow) but due to its proximity to the dominant band at 990 cm^{-1} , the significance of this band cannot be estimated from experimental data

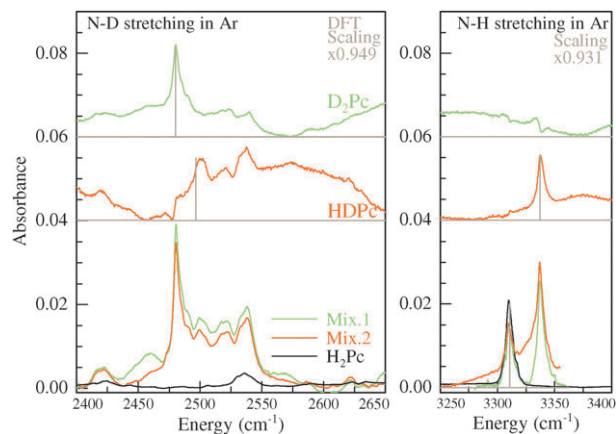


Fig. 5 Raw spectra of the two mixtures of H₂Pc, HDPc and D₂Pc in solid Ar obtained by synthesis 1 and 2 are shown in the lower section. The spectrum of 2 has been divided by a factor of 1.45 in order to make the intensities of the bands of H₂Pc and D₂Pc coincide. The absorption of a sample containing only H₂Pc is shown (in black) to allow identification of a combination mode at 2538 cm⁻¹. The upper section shows the difference spectra in the region of the N–D and N–H stretching modes of H₂Pc, HDPc and D₂Pc in an Ar matrix. The broad underlying curvature present in the two difference spectra is a result of working with two samples having slightly different thicknesses. DFT predictions are shown by the stick spectra and scaled by the indicated factors.

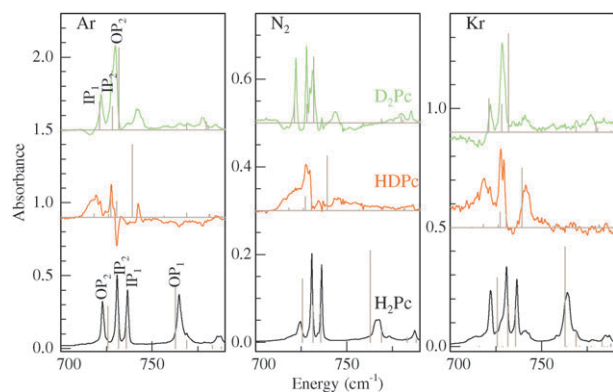


Fig. 6 Infrared spectra in the region of 700–800 cm⁻¹ of H₂Pc, HDPc and D₂Pc trapped in different solids (Ar, N₂ and Kr). The results of the DFT calculations on the three isotopomers are shown by the stick spectra scaled by 0.98. The labels OP and IP indicate out-of-plane and in-plane bending modes respectively. Particularly noteworthy is the mode labelled OP₂ whose frequency increases from the light (H₂Pc) to the heavy (D₂Pc) isotopomer.

alone. Another difficulty in the present attributions is the large intensity variations amongst the lines of the different isotopomers. The right panel in Fig. 7 presents the isotope dependence observed in the 1150–1300 cm⁻¹ region. The most pronounced effect exhibited here is the removal of the moderately intense band of H₂Pc at 1252 cm⁻¹ indicated by the black arrow. No new, well-defined feature is evident in D₂Pc; the occurrence of new bands is obscured by the residual in the difference spectra of the strong bands of H₂Pc.

The frequencies of the vibrational modes which shift most upon deuteration in solid Ar are reported in Table 4. No

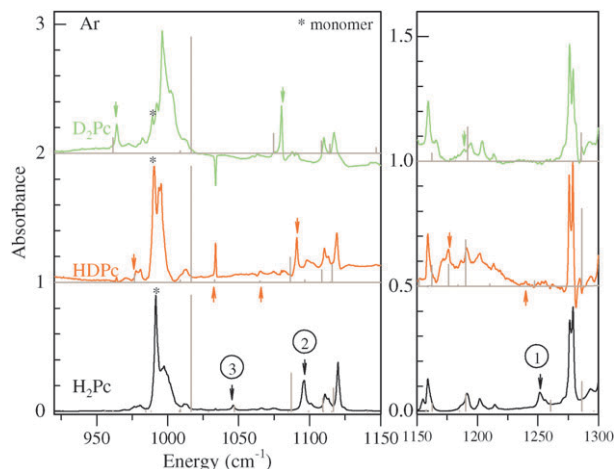


Fig. 7 Difference spectra of H₂Pc, HDPc and D₂Pc in an Ar matrix in the 900–1150 and 1150–1300 cm⁻¹ regions. The asterisks (*) around 1000 cm⁻¹ indicate the absorptions of fully isolated monomer molecules. As in the previous figure, scaled (×0.98) DFT results are shown for comparison purposes. The modes of H₂Pc exhibiting a significant dependence on isotopic substitution are numbered and discussed in detail in the text.

significant differences in the frequency shifts are detected in other matrices. In order to further investigate the observed isotope shifts and thereby obtain mode assignments of the IR absorption bands, theoretical predictions are required. More detailed comments on these experimental results will be presented in the Discussion.

Raman data for the deuterated species have been recorded in KBr pellets, with a D₂Pc sample containing some residual hydrogenated isotopomers. The corresponding spectrum is presented in Fig. 8 and compared with that of H₂Pc in KBr recorded under identical experimental conditions. The observed bands are reported in Table 2. The D₂Pc and H₂Pc Raman spectra are very similar, behaviour in agreement with the previous remark concerning the similarities between H₂Pc and ZnPc Raman spectra. The main differences involve the appearance of new weak bands at 986.1 and 1044.1 cm⁻¹, slight shifts of the 1227.8 and 1406.5 cm⁻¹ bands of H₂Pc to 1217.9 and 1402.2 cm⁻¹ for D₂Pc, respectively, and a structure in the strong band around 1340 cm⁻¹. The band around 1400 cm⁻¹ seems to shift with the sample preparation and is assigned to clusters or complexes. In contrast to the IR spectra, this is the only evidence we have identified in the Raman spectra for the presence of an aggregate band in KBr. As in the case of IR data, the isotope shifts in the Raman data will be discussed in the light of theoretical predictions obtained using DFT calculations.

B DFT calculations data

We used Density Functional Theory to generate force fields from the optimised molecular geometries of ZnPc and H₂Pc. Computed vibrational frequencies of ZnPc and the isotopomers H₂Pc, HDPc and D₂Pc were then analysed and compared with the recorded spectra to examine, in particular, the N–H vibrational modes.

Table 4 Comparison of the experimental IR frequencies recorded for free base phthalocyanine in an Ar matrix and DFT computed frequencies for the modes exhibiting the largest shifts upon H/D isotopic substitution. The intensities are given in parentheses as km mol^{-1} . A scaling factor of 0.98 has been used for all modes less than 2000 cm^{-1} . Larger scaling factors, as indicated, have been used for the higher frequency N–H stretching modes reflecting the larger anharmonicities of these modes. Experimental values shown in parentheses are either very weak or only partially resolved. Question marks indicate bands which were not identifiable in the recorded spectra

Exp.	Ar				DFT					Mode assignment
	H ₂ Pc	HDPc	D ₂ Pc	Shift	Shift ^a	H ₂ Pc	HDPc	D ₂ Pc	Shift	
722.7	719.3	729.9	−10.6	−7.2	725.7 (127)	718.2 (14)	731.8 (249)	−13.6	−6.1	C–H N–D OPB (doming) C–H N–H OPB (doming)
764.8	?	555	?	209.8	762.8 (184)	516.3 (4)	555.0 (18)	−38.7	207.8	N–D C–H OPB N–H C–H OPB
	742.5		22.3			739.3 (275)		23.5		
	727.6	722.1	5.5	14.5		727.4 (71)	721.2 (85)	6.2	14.6	N–D IPB, isoindole deformation
736.6	?		?		735.8 (68)	756.6 (4)		−20.8		N–H IPB, isoindole deformation
1046.2	977.8	964.1	13.7	82.1	1047.0 (29)	976.6 (45)	961.5 (89)	15.1	85.5	N–D IPB, pyrrole rocking N–H IPB, pyrrole rocking
	1033.6		12.6			1033.0 (15)		14		
	(1065.6)	1080.2	−14.6	15.9		1065.0 (8)	1074.6 (112)	−9.6	12.2	N–D C–H IPB isoindole stretching
1096.1	1090.9		5.2		1086.8 (217)	1086.2 (143)		0.6		N–H C–H IPB isoindole stretching
	(1176.1)	(1188.9)	18.5	62.9		1176.2 (14)	1192.0 (60)	−15.8	68.7	C–D N–D IPB, C–C stretching pyrrole
1251.6	(1240.4)		11.2		1260.7 (19)	1247.2 (3)		13.5		C–H N–H IPB, C–C stretching pyrrole
3310.0	2501.4	2480.5	20.9	829.5	3310.8 (134)	2496.7 (59)	2480.3 (113)	16.4	830.5	N–D stretching (×0.949)
	3337.1		−27.1			3337.3 (64)		−26.5		N–H stretching (×0.931)

^a Shift H₂Pc–D₂Pc.

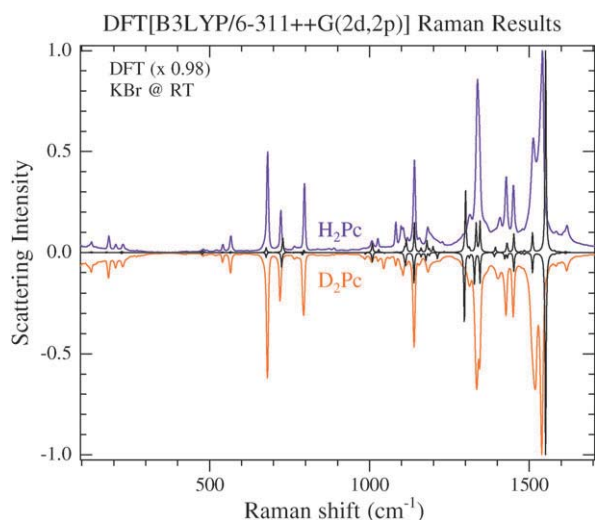


Fig. 8 A comparison of the Raman spectra recorded for H₂Pc and D₂Pc. The experimental data were recorded at room temperature in a KBr pellet with 532 nm excitation. The DFT predicted spectra (shown by the black traces) were obtained by convoluting the calculated lines with a 3 cm^{-1} Lorentzian lineshape function.

1 Optimised geometries. The geometries of ZnPc and H₂Pc were optimised in the D_{4h} and D_{2h} symmetries, respectively, and the fact that no negative frequencies were observed indicates that planar structures are predicted for the phthalocyanines with the 6-311++G(2d,2p) basis set used. This

result is in contrast to previous DFT calculations¹³ for ZnPc, in which a “domed” C_{4v} structure was found employing a smaller 6-31G(d,p) basis set. Full geometric details of the optimised structures of ZnPc and H₂Pc resulting from use of the B3LYP functional are presented as Table S1 in the ESI.† The atom labelling systems used for ZnPc and H₂Pc are those provided in Fig. 1. It is noteworthy that at this level of theory, the bond lengths in particular match the crystal data²⁵ better and are shorter than the previous highest level [6-311+G(d)] DFT calculation of ZnPc by Nguyen and Pachter.²⁶ A smaller improvement has been obtained for H₂Pc compared with the results of the recent high level [6-311++G(p,d)] calculation by Strenalyuk *et al.*²⁷

2 Vibrational modes. ZnPc with 57 atoms has 165 fundamental vibrational modes, which can be categorised as $A_{1u}(6)$, $A_{2u}(8)$, $B_{1u}(7)$, $B_{2u}(7)$, $E_u(28)$, $A_{1g}(14)$, $A_{2g}(13)$, $B_{1g}(14)$, $B_{2g}(14)$ and $E_g(13)$ in D_{4h} symmetry. H₂Pc, with one additional atom, has 168 fundamental vibrational modes and, with its reduced D_{2h} symmetry, yields $A_u(13)$, $B_{1u}(15)$, $B_{2u}(28)$, $B_{3u}(28)$, $A_g(29)$, $B_{1g}(28)$, $B_{2g}(14)$ and $B_{3g}(13)$ modes.²⁸ Due to their very close geometries, strong similarities exist between the vibrational modes of ZnPc and H₂Pc. From group theory correlations, the $A_{1u,g}$ [$A_{2u,g}$] and $B_{1u,g}$ [$B_{2u,g}$] modes of D_{4h} symmetry are merged in the $A_{u,g}$ [$B_{1u,g}$] modes of D_{2h} symmetry, respectively, and the degenerate $E_{u,g}$ modes of D_{4h} symmetry are split in $B_{2u,g}$ and $B_{3u,g}$ modes in D_{2h} symmetry. In this perspective, the additional modes of H₂Pc compared to

ZnPc are three *gerade* modes with A_g , B_{1g} and B_{2g} symmetries. In ZnPc (D_{4h}), only 36 u modes are infrared-active [A_{2u} and E_u modes] while 55 g modes [A_{1g} , B_{1g} , B_{2g} and E_g modes] are Raman-active. The corresponding numbers in H_2Pc (D_{2h}) are 71 infrared-active u modes [$B_{1u}(15)$, $B_{2u}(28)$ and $B_{3u}(28)$], and 84 Raman-active g modes [$A_g(29)$, $B_{1g}(28)$, $B_{2g}(14)$ and $B_{3g}(13)$].

Harmonic frequencies have been calculated for the normal modes of ZnPc, H_2Pc and its isotopomers HDPc and D_2Pc . Frequency values for all the vibrational modes of ZnPc, H_2Pc and D_2Pc are provided in the ESI† in Table S2 for the infrared-active modes and in Table S3 for the Raman-active modes. The 13 optically inactive modes (data not provided) are found to be exactly similar in H_2Pc and D_2Pc , with only very small shifts in frequencies between free-base and zinc phthalocyanine. An effort was made in these tables to arrange the corresponding modes of the three species on the same lines. This mode association has been achieved with the assistance of the animated pictures generated by Gaussian 03 for the normal modes. All u modes have g counterparts in the same range of frequencies—these modes correspond to the same bond motions but with different symmetries. For instance DFT results indicate that the intense IR modes in the 1100 to 1200 cm^{-1} range arise from the IP bending modes of the aryl ring-C-H bonds. This finding is supported by the pronounced isotope shifts observed by Gladkov *et al.*²⁹ in the Raman spectra of ZnPc- d_{16} in KBr pellets.

The correspondence between the vibrational modes of zinc and free-base phthalocyanine is in most cases very clear, especially for the B_{3u} , A_g , B_{2g} and B_{3g} symmetry modes of the free-base. The three additional *gerade* modes are found, as expected, to be strongly influenced by NH(D) motions. With the assistance of animated pictures, it is obvious that fifty–fifty mixtures of ZnPc A_{1g} and B_{1g} C-H stretching modes are correlated to H_2Pc A_g C-H stretching modes. Correlations

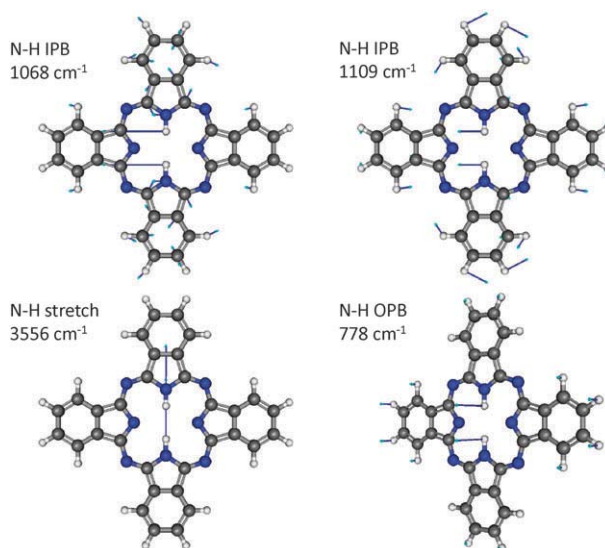


Fig. 9 Vector displacement representations of the N–H vibrations of H_2Pc calculated with the DFT method for the most intense IR absorptions. The diagrams depict the extent of the coupling between the N–H bends and bending of the C–H bonds on the aryl groups. In contrast, the N–H stretch can be considered a pure, isolated motion. The frequencies provided are the unscaled DFT calculated values.

are much less evident in the case of the In-Plane Bending modes (ZnPc E_u , A_{2g} and B_{2g} modes) between 1000 and 1500 cm^{-1} when the N–H(D) In-Plane bending motion of the free-base perturbs the ring motions (see Part C of the Discussion). The frequency ratios (ν_H/ν_D) calculated for the vibrational modes of H_2Pc and D_2Pc highlight the involvement of N–H motion on the modes. Table 5 presents a summary of the computed frequency modes involving a ν_H/ν_D ratio significantly different from unity.

Table 5 The vibrational modes of H_2Pc exhibiting the largest isotopic shifts upon H–D substitution according to DFT calculations. For comparison, the vibrational frequencies of ZnPc are also provided. The predicted intensities are given in parentheses for both IR ($km\ mol^{-1}$) and Raman ($A^4\ amu^{-1}$) transitions. The values given in italics are ambiguous correlations between free bases and phthalocyanines. The values in bold correspond to the highest ν_H/ν_D ratio

IR modes				Raman modes			
ZnPc ν (int)	H_2Pc ν (int)	D_2Pc ν (int)	ν_H/ν_D	ZnPc ν (int)	H_2Pc ν (int)	D_2Pc ν (int)	ν_H/ν_D
Out-of-plane bending							
A_{2u}		B_{1u}		E_g		B_{2g}	
250 (0)	217 (7)	214 (8)	1.0143	235 (2)	220 (3)	214 (3)	1.0276
749 (247)	740 (127)	747 (249)	0.9916	509 (0)	506 (0)	511 (0)	0.9891
123 (11)	778 (184)	566 (18)	1.3744		680 (0)	495 (0)	1.3738
797 (31)	804 (5)	796 (24)	1.0105				
In-plane bending							
E_u		B_{2u}		$A_{2g} + B_{2g}$		B_{1g}	
511 (8)	499 (2)	489 (1)	1.0197	589 (0)	580 (2)	563 (2)	1.0305
768 (61)	751 (68)	736 (85)	1.0202	629 (0)	612 (1)	600 (0)	1.0212
906 (56)	855 (0)	779 (2)	1.0969	864 (0)	841 (I)	880 (0)	0.9563
1111 (174)	1068 (29)	981 (89)	1.0889	1057 (116)	1050 (228)	1007 (134)	1.0422
1084 (154)	1109 (217)	1096 (112)	1.0114	964 (42)	1107 (43)	1068 (65)	1.0360
1190 (30)	1181 (2)	1170 (32)	1.0096	<i>1157 (0)</i>	<i>1224 (520)</i>	<i>1191 (59)</i>	<i>1.0270</i>
250 (5)	1286 (19)	1216 (60)	1.0576	<i>1232 (741)</i>	<i>1259 (73)</i>	<i>1237 (536)</i>	<i>1.0173</i>
<i>1360 (234)</i>	1568 (8)	1546 (2)	1.0142	1485 (0)	1566 (3)	1550 (14)	1.0105
In-plane stretching							
E_u		B_{3u}		$A_{1g} + B_{1g}$		A_g	
250 (5)	3556 (134)	2614 (113)	1.3606	—	3612 (13)	2649 (36)	1.3634

The assignment of N–H(D) stretching modes is straightforward for both the B_{3u} and A_g symmetry groups, with only one mode yielding a large ν_H/ν_D ratio of 1.36, close to $\sqrt{2}$. Theoretically predicted values are 3556 [2614] and 3612 [2649] cm^{-1} for N–H[D] u and g stretching modes respectively. The former values when scaled by 0.931 [0.949] are in excellent agreement with the previously described IR experimental values. The symmetric Out-of-Plane Bending (OPB) NH(D) modes (B_{1u} and B_{2g}) also show a similarly high isotopic ratio (1.37) providing a clear assignment 778 [566] and 680 [495] cm^{-1} for the N–H[D] u and g OPB modes respectively. Conversely, only ratios close to one are obtained in the case of the In-Plane Bending (IPB) NH[D] modes (B_{2u} and B_{1g} symmetry). Thus it would appear that there is no normal mode in H_2Pc corresponding to a pure IPB motion of the NH groups alone. As mentioned in the previous work of Zhang *et al.*,¹⁴ this motion is strongly coupled with the ring breathing modes. Fig. 9 illustrates the extent of the coupling between IP bending of the aryl C–H bonds and the N–H bending motions, whereas the N–H IP stretching modes exhibit pure motions. At least eight IPB modes of each symmetry are affected by deuteration. This coupling of the N–H IP bending with other motion is especially strong for the *gerade* modes for which correlations between H_2Pc and D_2Pc (and ZnPc) modes are difficult to establish. From animated pictures, the IPB modes involving the largest NH bending motion (H_2Pc) are identified at 1286 (B_{2u}) and 1107/907 cm^{-1} (B_{1g}), and those involving the largest ND bending (D_2Pc) are at 981 (B_{2u}) and 763 cm^{-1} (B_{1g}). These frequencies are located in a dense part of the vibrational manifold of free-base phthalocyanine.

IV. Discussion

A IR absorption

The computed IR absorption spectrum of ZnPc is compared scaled by a factor of 0.98 in the upper panel of Fig. 10 with

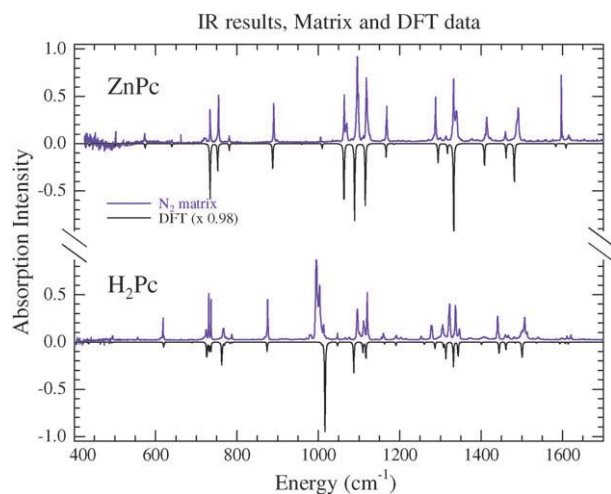


Fig. 10 A comparison of the observed and the DFT predicted infrared absorption spectra for ZnPc (upper panel) and H_2Pc (lower panel). The experimental data were recorded at 14 K in a nitrogen matrix while the predicted values were obtained with a DFT calculation using the B3LYP functional and a 6-311++G(2d,2p) basis set. The theoretical lines have been convoluted with a 1 cm^{-1} Lorentzian lineshape.

that recorded in a N_2 matrix where the close agreement that exists, both in terms of the band positions and the band intensities, is quite evident. Very significant improvement was obtained by increasing the basis set from 6-31G(d,p) to 6-311++G(2d,2p)—an indication of the importance of having polarisation functions present. This basis set yields much better agreement in the region up to 1000 cm^{-1} than what Tackley *et al.*¹³ achieved with the 6-31G(d,p) basis comparing with data recorded for ZnPc in KBr discs. Calculated frequencies are compared to experimental results in Table 1. In the 400–1650 cm^{-1} spectral range, almost all the lines with a calculated intensity larger than 3 km mol^{-1} are observed and assigned. The symmetries of the modes listed in the last column were assigned through DFT calculations. Only two of the well observed bands (reported for KBr pellets at 727 and 782 cm^{-1}) correspond to out-of-plane modes.

Two of the three C–H stretching modes have much larger computed intensities than the other. According to this finding, the clearly observed doublet located at 3072.3 and 3093.5 cm^{-1} in N_2 should be assigned to these two modes. The additional structures in the spectra shown in the upper panel of Fig. 3 are probably due to site effects in the matrix. A third weaker but clearly identifiable band at 3038.3 cm^{-1} is attributed to a strong combination band. The third (weakest) C–H stretching mode, which has not been resolved in the matrix spectra, is probably a shoulder on the red wing of the 3072.3 cm^{-1} band.

In the lower panel of Fig. 10 the matrix and computed IR spectra of H_2Pc are compared. As found for ZnPc , excellent agreement exists below 1000 cm^{-1} but is not quite as good in the region above this. From a combination of the increased number of optically active modes in H_2Pc and the removal of the degeneracy of the E modes of ZnPc , free-base phthalocyanine is expected to have a significantly richer vibrational spectroscopy than its metal-counterparts, and indeed, the IR H_2Pc spectrum exhibits more resolved lines than ZnPc . Nevertheless, due to their similar geometries, a close correspondence exists between the modes of both molecules as illustrated in Fig. 10, except around 1000 cm^{-1} .

While the IR spectrum of ZnPc is dominated by three nearly equivalent strong bands between 1000 and 1200 cm^{-1} (1063.6, 1095.9 and 1117.8 cm^{-1} in N_2) only a single intense feature is present in the free-base spectrum slightly below 1000 cm^{-1} . The strongest band in the calculated free-base spectrum is located at 1016 cm^{-1} (scaled) and from its dominant intensity, this mode must correspond to the most intense band observed at 995.0 (991.5) cm^{-1} in N_2 (Ar) spectra. The additional structure on the blue side of the recorded band is attributed to the presence of small amounts of aggregates present in the matrix samples.

Correlations deduced from DFT calculations (Table S2, ESI[†]) indicate that the 1117.8 cm^{-1} band of ZnPc in N_2 (E_u symmetry) splits into the 1112.4 and 1120.6 cm^{-1} bands of H_2Pc in N_2 (B_{3u} and B_{2u} symmetry, respectively) with moderate intensities. In contrast, the 1063.6 cm^{-1} band of ZnPc in N_2 corresponds only to one band of H_2Pc located at 1096.0 cm^{-1} in N_2 (B_{2u} symmetry) while in the case of the free base, the corresponding B_{3u} mode shows almost no IR intensity. Conversely, the most intense free-base B_{3u} mode located at 995.0 cm^{-1} in N_2 is correlated with the third

component in the ZnPc/N₂ spectrum at 1095.9 cm⁻¹. The B_{2u} counterpart mode of the free base, located at 1047.1 cm⁻¹ in N₂, is a weak line which disappears upon deuteration. Of the IPB modes, this motion involves pronounced N–H bending—it occurs, see Fig. 9, in combination with in-plane stretching of the C_α–N–C_α bonds in the two pyrrole rings that contain N–H bonds (calculated at 1068 cm⁻¹ in Table 5).

The corresponding B_{3u} component (995 cm⁻¹ in N₂) mode does not involve N–H motion, but is an in-plane stretch of the C_α–N–C_α bonds in the two pyrrole rings (see Fig. 1) that do not contain N–H bonds. This mode of the monomer is, as shown by the asterisks in Fig. 7, only marginally shifted in HDPc and D₂Pc, entirely consistent with DFT findings. A similar finding was made by Zhang *et al.*,¹⁴ based on a comparison between predicted MgPc and H₂Pc spectra. The large shift of the strong mode not having N–H motion explains the long-standing conflicting behaviour that the new mode of H₂Pc (which is not present in ZnPc) shows no dependence on H/D isotope substitution. The present DFT calculations, including the results obtained for the metallo-phthalocyanine ZnPc, strongly confirm the mode assignments and fully explain the unexpected isotope behaviour.

In the C–H stretching region, the recorded IR spectra of the free-base and ZnPc are very similar as shown in Fig. 3. DFT calculations for H₂Pc predict a splitting of the three bands occurring for ZnPc. This splitting, arising from the reduced symmetry in the free-base, is however not evident in the recorded matrix spectra. Details of NH deuteration effects on the IR spectra will be discussed in Part C.

B Raman scattering

The computed Raman spectra of ZnPc and H₂Pc are compared with those recorded at room temperature in KBr discs in Fig. 11, and all the computed peak positions are collected in Table 2. It is evident from these comparisons that

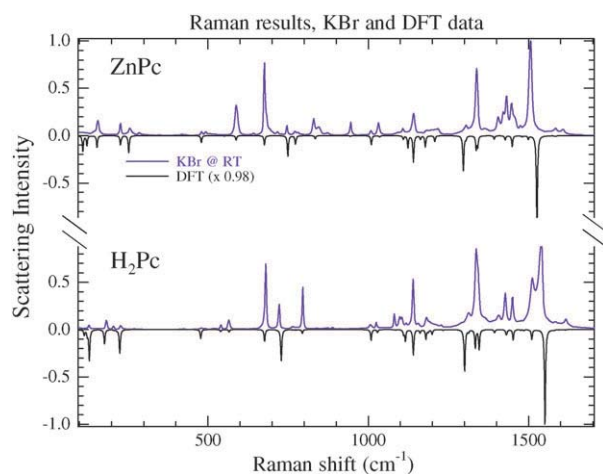


Fig. 11 A comparison of the observed and calculated Raman spectra for ZnPc (upper panel) and H₂Pc (lower panel). The experimental data were recorded at room temperature in a KBr pellet with 532 nm excitation. The predicted spectra were obtained by transforming the computed Raman activities to Raman intensities with the method outlined in the text. The theoretical lines have been convoluted with a 3 cm⁻¹ Lorentzian lineshape.

very good positional agreement exists in the case of both molecules. A noteworthy distinction between absorption and scattering spectroscopies of the phthalocyanines is that both in-plane and out-of-plane motions are IR-active while only the in-plane vibrations are readily observed in Raman spectra. The out-of-plane E_g modes of ZnPc, which although allowed by group theory, are predicted to be extremely weak. In the computed Raman spectrum, the in-plane A_{1g} and B_{1g} modes carry most of the intensity while the B_{2g} modes are much weaker. Similarly, for H₂Pc only two in-plane [A_g and B_{1g}] mode symmetries are found to exhibit significant Raman activities. As a result of this intensity behaviour, it is found that only a limited number of modes dominate the recorded Raman spectra of both molecules. The Raman modes fall mainly into two categories, those involving motion of the central ring and those of the aryl and pyrrole parts of the isoindole groups.

DFT predictions for the Raman intensity seem to be much less accurate than frequency predictions. For instance, assignment of the strong Raman band of ZnPc (H₂Pc) at 1338.3 (1336.7) cm⁻¹ is not straightforward. From DFT calculations, the most intense band in this range is predicted at 1296.5 (1300.5) cm⁻¹, whereas, from frequency positions, the experimental band could be assigned to either the 1336.5 (1333.7) or 1341.5 (1345.8) cm⁻¹ predicted bands, or the sum of both. From the structure observed in the case of D₂Pc in KBr, the last assignment is preferred as it is consistent with the observation, depicted in Fig. 8, that the predicted spectral shift between these two modes is larger for D₂Pc than for H₂Pc. According to this attribution, the second most intense predicted Raman band of H₂Pc at 1300.5 cm⁻¹ (scaled) corresponds, as shown in Table 2, to the observed shoulder at 1293.7 cm⁻¹. This assignment is consistent with the isotopic shift observed in D₂Pc where the shoulder is observed at 1290.8 cm⁻¹ and the predicted value is at 1296.5 cm⁻¹ (scaled). A possible reason for the intensity discrepancies between the predicted and observed Raman spectra arises from small contributions from resonance effects. This was examined in the earlier work by Tackley *et al.*,¹⁵ who chose a range of laser excitation wavelengths from 457 to 1064 nm to record Raman spectra of ZnPc.

The main discrepancy between the experimental frequencies and their DFT predicted values concerns the positions of the two most intense Raman bands located at 1539.5 cm⁻¹ (H₂Pc) and 1506.8 cm⁻¹ (ZnPc). For ZnPc the strongest band is predicted 19 cm⁻¹ higher than the observed band while in H₂Pc it is 12 cm⁻¹ higher. The attributions given in Table 2 for the strongest predicted Raman lines in ZnPc and H₂Pc spectra are unavoidable due to the clear dominance of these bands in both theory and experiment. Previous calculations by Liu *et al.*³⁰ for ZnPc and Strenalyuk *et al.*²⁷ for H₂Pc found even larger discrepancies for these modes. It is worth mentioning that this small lack of agreement between theory and experiment on the most intense Raman mode has been found in the high level calculations³¹ of all the Pcs (H₂Pc, ZnPc, MgPc and AlPc) for which we have Raman data. We have nevertheless observed that increasing the size of the basis set leads to improved agreement for these B_{1g}/A_g modes for both ZnPc and H₂Pc. On the other hand, the existence of well-resolved

bands at 3080 and 3012 cm^{-1} in the Raman spectra of H_2Pc and ZnPc , respectively, can be readily attributed to first overtones of the strongest fundamental modes at 1539.5 and 1506.8 cm^{-1} . As the difference between the observed overtones and the values predicted by simply doubling the fundamental frequencies is so small (*ca.* 1 cm^{-1}) it can be concluded that the anharmonicities of these modes are small.

The most intense 1506.8 and 1539.5 cm^{-1} Raman modes of ZnPc and H_2Pc , respectively, are of considerable significance since their frequencies shift with the metal centre and as a result, they have been proposed¹⁵ as spectroscopic markers of the ring size in the Pcs. They are of particular interest to us, because these are the modes which exhibit amplified emission with pulsed laser excitation.⁵ DFT calculations reveal that this mode involves the same motion in both ZnPc and H_2Pc corresponding to the antisymmetric stretch of the four bridging $\text{C}_\alpha\text{-N}_m\text{-C}_\alpha$ bonds and symmetric stretching of the $\text{C}_\alpha\text{-N}_{\text{zn(H)}}\text{-C}_\alpha$ bonds in the four pyrrole groups (see Fig. 1). From these descriptions, it is clear that this normal mode involves stretching of all 16 C–N bonds in the central ring of the tetrapyrrole.

The first overtones of the strong fundamentals in the 1300 to 1550 cm^{-1} range make it difficult to locate the positions of the weak symmetric fundamental C–H stretching modes of both ZnPc and H_2Pc in the experimental spectra. Symmetric and antisymmetric C–H stretching modes are predicted with very similar frequencies. By eliminating easily identifiable overtone bands and with the help of DFT calculations, the strongest Raman active C–H mode of ZnPc can be identified at 3086.9 cm^{-1} . The corresponding band of H_2Pc has not been identified as it is overlapped by a stronger (factor of 20) overtone band at 3080 cm^{-1} as shown in the panel on the right in Fig. 4.

C Isotope shifts

Table 5 summarizes the vibrational modes influenced by N–H deuteration as predicted by DFT calculations. One can notice that theoretically none of these modes exhibit strong Raman activity. In particular, no N–H out-of-plane modes are predicted to be observable in the Raman spectrum. Fortunately, the new IR experimental data give much more information on these modes. In the D_{2h} point group, only the B_{1u} , B_{2u} and B_{3u} symmetry modes are infrared active. These are the symmetries of the out-of-plane N–H bend (NH-OPB), the in-plane N–H bend (NH-IPB) and the antisymmetric N–H stretch modes respectively. DFT values reported in Table 5 indicate that these three kinds of modes (in u and g symmetries) should appear in three distinct spectral ranges 500–800 cm^{-1} , 800–1300 cm^{-1} and around 2500 (D)/3500 (H) cm^{-1} respectively. Table 4 summarizes the IR experimental isotopic shifts compared with DFT calculations, allowing a more complete description of these modes.

1 N–H stretching modes. The antisymmetric N–H stretching mode has been identified at 3290 cm^{-1} in KBr pellets¹² and at 3273 cm^{-1} in Nujol.¹² This assignment has been supported by the observation of the N–D antisymmetric stretching at 2458 cm^{-1} . Our matrix results also confirm this assignment with the N–H stretching mode of H_2Pc observed in

Ar (see Fig. 3) at 3310 cm^{-1} while the N–D stretching mode of D_2Pc is at 2480.5 cm^{-1} . For a molecule such as HDPc with C_{2v} symmetry, the N–H and N–D bonds are inequivalent and both stretches are expected. Accordingly, the N–H stretch mode of HDPc is observed at 3337.1 cm^{-1} while the N–D stretch is at 2501.4 cm^{-1} . It is clear in Table 4 that the experimental and calculated shifts for the N–H stretching modes in H_2Pc and HDPc are in very good agreement. The same can be said for the shift of the N–D stretching modes in HDPc and D_2Pc .

As previously mentioned, the symmetric N–H stretching vibration of H_2Pc (the highest frequency fundamental mode) is predicted to be only very weakly Raman active but the present KBr spectra do show a weak band at 3343 cm^{-1} which could be identified as this stretching mode. Its location is indicated by the arrow in Fig. 4. A slightly more pronounced band is observed in the Raman spectrum of D_2Pc at 2504.7 cm^{-1} which can be assigned to the symmetric N–D stretching mode. This is in agreement with DFT results but the location of this N–D mode is in a spectral region where stronger combination and overtone bands render its identification difficult.

2 In-plane bending (NH-IPB) modes. Because of its absence in KBr IR spectra of metal-phthalocyanines, Shurvell and Pinzuti¹¹ assigned the most intense band of H_2Pc at 1006 cm^{-1} to an N–H deformation. However, this assignment to the N–H bending mode appears now to be incorrect for the reasons presented previously in Part A. Consistent with experiments, DFT calculations show the corresponding unscaled band (with B_{3u} symmetry) at 1037.22 cm^{-1} in H_2Pc and at 1037.12 cm^{-1} (unscaled) in D_2Pc .

As mentioned in Part A, DFT calculations reveal that the corresponding B_{2u} mode occurs at a higher frequency but with greatly reduced intensity. In H_2Pc it is predicted at 1068.4 cm^{-1} (unscaled) and weaker by a factor of more than 20 relative to the most intense mode in the IR spectrum. The corresponding mode in D_2Pc is located at 981.15 cm^{-1} (unscaled) but stronger by a factor of 4 than its H_2Pc counterpart. The locations of these modes in Ar are indicated in Fig. 7 by the arrows (and numbered 3) while the stick spectra present the scaled ($\times 0.98$) DFT-predictions. This band was found to exhibit the largest shift upon deuteration among the observed IPB modes. The agreement, evident in Fig. 7, between experiment and theory for the isotope dependence of this mode is excellent. The N–D IPB mode of HDPc is located at 977.8 cm^{-1} , consistent with scaled DFT predictions, but the N–H IPB mode of HDPc (predicted at 1033 cm^{-1} with a very low intensity) is masked by an artefact of the difference method used in generating the spectrum shown. The most likely position of the mode of HDPc is indicated by the upward arrow on the left in Fig. 7.

In a molecule as large as phthalocyanine, it is important to remember that the vibrational modes are strongly coupled and only the N–H (and N–D) stretching vibrations can be considered to be a pure motion. This coupling is the primary reason why so many different assignments of NH-OPB and NH-IPB modes have been made because attributing them to the experimentally observed modes is not direct. This difficulty is especially severe in the case of the N–H IPB modes. An indication of the strongly coupled nature of the N–H-bending

modes is depicted in the vector diagrams presented in Fig. 9. As a result, none of the mode correlations yield a $\nu_{\text{H}}/\nu_{\text{D}}$ ratio larger than about 1.1.

The highest frequency N–H IP bending mode we have found in DFT calculations of H₂Pc is at 1567.89 cm⁻¹ which shifts only to 1545.9 cm⁻¹ in D₂Pc. The vibrational frequencies calculated by Zhang *et al.*¹⁴ with the smaller 6-31G* basis set are lower—at 1533 cm⁻¹ for H₂Pc, shifted to 1514 cm⁻¹ in D₂Pc—but consistent with our findings. The reason for the small $\nu_{\text{H}}/\nu_{\text{D}}$ ratio of 1.014 for this mode becomes evident from the vector displacement diagram where it is clear that this mode is primarily stretching of the bridging C _{α} –N_m–C _{α} bonds—a motion which only secondarily induces NH-IP bending. Dispersion of the NH-IP bending mode amongst this and other stretching vibrations reduces the $\nu_{\text{H}}/\nu_{\text{D}}$ ratio making this mode very difficult to identify in isotope substitution work. Moreover, the mode at 855 [779] cm⁻¹, which corresponds to the most pronounced deuteration effect in the *ungerade* NH IPB modes, is also predicted to have a vanishingly small IR activity.

Five of the N–H IPB modes reported in Table 5 are observed in IR matrix spectra of H₂Pc, but only the four located at 1251.6, 1096.1, 1046.2 and 736.6 cm⁻¹ in Ar are, with the help of DFT calculations (see Table 4), intense enough to be followed upon deuteration. The first of these is numbered (1) and marked by an arrow in the panel on the right of Fig. 7. The assignments given for the bands in the HDPC spectrum are only tentative as the predicted IR intensities are very weak for this mode. The second mode, involving a small isotopic shift from 1096.1 for H₂Pc to 1080.2 cm⁻¹ for D₂Pc in Ar, is the most intense and is clearly observed as indicated by number 2 in the left panel of Fig. 7. In the HDPC case only the NH component at 1090.9 cm⁻¹ in Ar is intense. The third one was discussed above and is marked by arrows and numbered 3 in Fig. 7. The last one present at 736.6 cm⁻¹ is included in the spectral range corresponding to NH OPB modes and is indicated as IP₁ in Fig. 6. According to DFT predictions, this mode appears at 722.1 cm⁻¹ for D₂Pc and at 727.6 cm⁻¹ for HDPC in Ar. Only one of the two predicted components of HDPC has a significant intensity.

Five of the symmetric N–H IPB modes are observed with weak intensities in Raman spectra. Their frequencies are given in Table 2 at 888.9, 1025.5, 1081.4, 1190, and 1227.8 cm⁻¹ while their unscaled DFT values are listed in Table 5 as 907, 1050, 1107, 1223 and 1259 cm⁻¹. According to DFT calculations, the deuterated counterpart of the first band should be located at 747.7 cm⁻¹ (scaled) but is not distinguishable in the D₂Pc spectrum. In contrast, two of the new bands observed for D₂Pc at 986 and 1044 cm⁻¹ are the deuterated counterparts of the two following bands. The fourth band at 1190 cm⁻¹ does not appear in the D₂Pc spectrum, and the fifth band is slightly shifted to 1219.5 cm⁻¹ in the deuterated sample, in very good agreement with theoretical predictions. These observations³² reinforce the assignment of these bands to *gerade* NH IPB modes. As most of the modes involving Raman activity are present in fluorescence spectra, these results can also be related to the emission work of Shkirman *et al.*³³ They show that deuteration of H₂Pc had only a weak effect on the fluorescence, consistent with the findings of the

present Raman spectra and DFT computations. Shkirman *et al.* noted the disappearance of a mode at 1357 cm⁻¹ together with the appearance of a mode at 990 cm⁻¹ upon H/D substitution. The assignment of the first mode to H₂Pc is doubtful, because it is absent in our experiments and calculations, but the mode at 990 cm⁻¹ is in a perfect agreement with the Raman active ND IPB modes measured at 986.1 cm⁻¹ (1007 cm⁻¹ in Table 5).

3. Out-of-plane bending (NH-OPB) modes. The anti-symmetric NH-OPB mode has previously been assigned to several bands in the 710–760 cm⁻¹ range. According to Shurvell and Pinzuti¹¹ it is the band at 716 cm⁻¹, while Sammes¹² identified it as the band at 735 cm⁻¹, which shifts to 549 cm⁻¹ in D₂Pc. However, as shown in Fig. 2 this spectral region is extremely complex in KBr spectra due to the presence of multiple bands, most of which are cluster related. In our matrix spectra, only a single H₂Pc band clearly disappears in this region upon deuteration. As shown in Fig. 6 this is the 764.8 cm⁻¹ band (labelled OP₁) of H₂Pc in Ar. In contrast to the IP bending modes, DFT calculations predict a clear correlation for the OP bending modes between the high frequency modes in H₂Pc and the low frequency modes in D₂Pc. Thus for one specific IR mode of H₂Pc at 778.36 cm⁻¹ a shift to 566.3 cm⁻¹ (unscaled values) is expected as indicated in Table 5. For this reason we assign the band around 765 cm⁻¹ as the main NH-OPB mode of H₂Pc. In Ar the band of HDPC shifts to 742.5 cm⁻¹, in agreement with the DFT calculations showing an unscaled frequency of 754.4 cm⁻¹ for the only HDPC OP mode with a large IR intensity in this region. The calculated frequency for the ND-OPB mode in D₂Pc (566.3 cm⁻¹ unscaled) is in good agreement with earlier predictions of Zhang *et al.*¹⁴ Unfortunately, the D₂Pc mode is so weak that it is not easily detected. However, a very weak band has been observed in an Ar matrix at 555 cm⁻¹. On the other hand, a weak new band at 777.8 cm⁻¹ appears in D₂Pc spectrum, it corresponds to the unobserved band calculated at 804 cm⁻¹ (788 cm⁻¹ scaled) for H₂Pc.

Fig. 6 shows a triplet centered at 730 cm⁻¹ in the H₂Pc spectrum, becoming very complex in HDPC and congested in D₂Pc spectra. The most intense component at 731 cm⁻¹ in Ar (labelled IP₂ in Fig. 6) is assigned to a B_{3u} mode and is nearly unshifted upon deuteration. It produces, as shown in Fig. 6, one part of the broad, structured feature in HDPC and D₂Pc. The highest energy component is the NH IPB mode discussed in the previous part (IP₁), shifting from 736.5 to 727.6 to 722.1 cm⁻¹ from H₂Pc to HDPC to D₂Pc in Ar. This band constitutes the lowest frequency component of the D₂Pc spectrum. The last component of the triplet (OP₂ at 722.8 cm⁻¹ in Fig. 6) at the lowest frequency in the H₂Pc spectrum is another NH OPB mode. As reported in Table 5 it is affected by deuteration but in an unexpected way. This mode is predicted at 732 cm⁻¹ (scaled) in D₂Pc, *i.e.* at the same frequency as the B_{3u} mode, explaining the experimental broadening (or structure in N₂) of this band. A comparison of scaled ($\times 0.98$) DFT frequencies is presented in Fig. 6 with the recorded spectra showing very close agreement.

A surprising finding of the present and Zhang's earlier¹⁴ DFT calculations is that this last N–D OP bending mode of

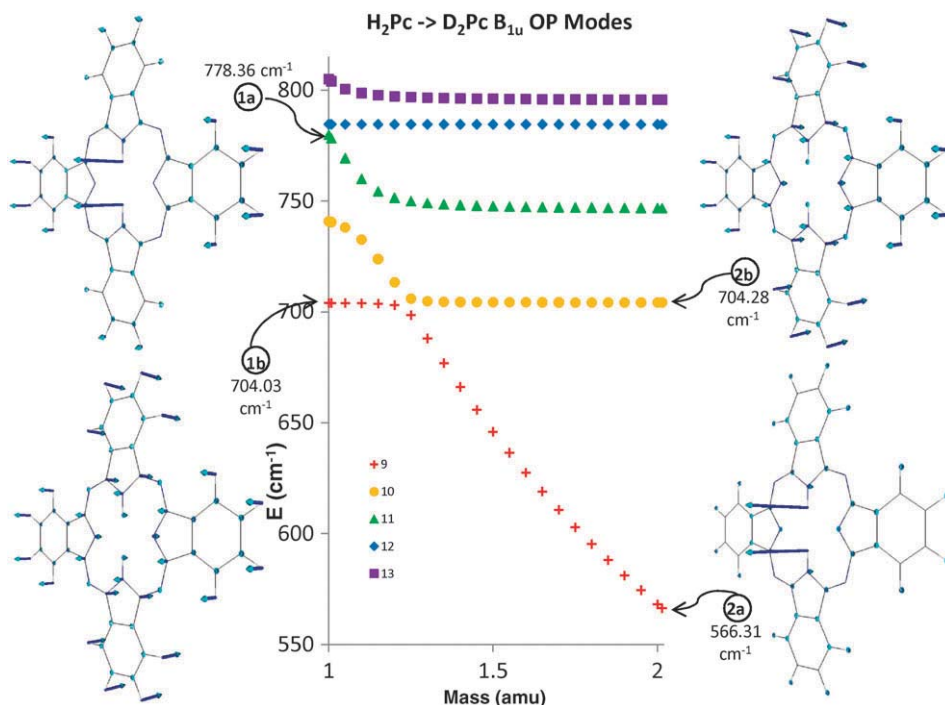


Fig. 12 DFT predictions of the isotope dependence of the IR-active OPB B_{1u} modes in H_2Pc and D_2Pc calculated at 0.05 amu increments. The vector displacements, two of which are shown on either side of the plot, were used in establishing the correlations. The numbering of the modes shown in the legend corresponds to that provided in Table S2 (ESI†).

D_2Pc is predicted at a higher frequency than the corresponding mode of H_2Pc . Such behaviour is predicted for a few other modes, as revealed in Table 5. An analysis of this unexpected behaviour now follows.

4 Inverse isotope substitution effects. In order to correlate the complex frequency shifts of H_2Pc and D_2Pc , the DFT computed frequencies were generated by increasing the masses of the two central hydrogens from 1 to 2 amu in increments of 0.05 amu. The results of this calculation are shown in Fig. 12 for B_{1u} symmetry between 550 and 850 cm^{-1} . The correlations were made by visually inspecting the vector displacement diagrams, four of which are presented in the figure.

From the vector diagrams shown in Fig. 12, it is evident that the purest N–H OPB modes in H_2Pc is located at 778.4 cm^{-1} (unscaled) which shifts down to 566.3 cm^{-1} in D_2Pc . This correlation results in the expected (within the accuracy of the DFT calculation) ν_H/ν_D ratio of 1.374 for H/D isotope substitution in a “pure” N–H mode. The large frequency shift of the pure NH-OPB mode results in it crossing several other out-of-plane bending modes. These crossings are more or less avoided depending on the coupling between modes. In Fig. 12, it is clear that there is almost no avoided crossing with the mode at 704 cm^{-1} which, as shown, involves no NH bending. In contrast, there is a strong avoided crossing with the mode at 740 (747) cm^{-1} in H_2Pc (D_2Pc). These values when scaled by 0.98 (725.7 and 731.8 cm^{-1} in H_2Pc and D_2Pc respectively) correspond to the resolved bands at 724.7 (H_2Pc) and 730.9 cm^{-1} (D_2Pc) in N_2 , shown in the middle panel of Fig. 6. The isotope frequency shift of this mode, labelled OP_2 , is depicted in the panel on the left of Fig. 6 for data

recorded in Ar. A consequence of this avoided crossing is that the 740 cm^{-1} H_2Pc mode exhibits the unusual behaviour of having an increased frequency (747 cm^{-1}) in the heavier isotopomer.

Even though this is a small upward shift ($\nu_H/\nu_D = 0.992$) it greatly complicates the recorded spectra as it occurs in the region where two strong in-plane modes of H_2Pc (D_2Pc) are located at 730.9 (728.0) and 736.4 (722.1) cm^{-1} in N_2 . Contrary to expectation, the mode-crossing results in the lowest frequency mode (OP_2) of the 730 cm^{-1} H_2Pc triplet, shifting up to the highest frequency mode of the D_2Pc triplet. These calculations show clearly that the triplet in D_2Pc involves an NH-OPB mode but distinct from the two strong bands in HDPc and H_2Pc at 742.5 and 764.8 cm^{-1} (values in Ar) respectively.

The last important avoided crossing evident in Fig. 12 is located near the mass 1 (H_2Pc). In fact, while the 566 cm^{-1} mode of D_2Pc involves almost pure ND motion, the 778 cm^{-1} mode of H_2Pc also exhibits CH bending motions. Similar curvature is present for the weak IR active mode of H_2Pc at 804 cm^{-1} . The motion of this vibrational mode is depicted in Fig. S3 (ESI†) as is the corresponding 796 cm^{-1} mode of D_2Pc . This curvature indicates that the coupling of the N–H(D) bending motions appears only in the vicinity of mass 1.

Such correlation diagrams have been calculated for the modes of all the symmetry groups. The results are presented in Fig. S2 of ESI† in the spectral range of the NH OP and IP bending modes (B_{1u} , B_{2u} , B_{1g} , B_{2g} symmetry groups). Whereas few crossings occur between masses 1 and 2 for OPB modes, the diagrams are much more complex for IPB modes, involving both large avoided crossings and traversal of un-coupled modes. In all cases where a ν_H/ν_D ratio of less than 1 occurs, it

is evident from the mode correlation diagrams that it results from avoided crossings. Moreover, the vector displacement diagrams reveal that in these cases, the direction of the N–H bending motion changes between the light and the heavy isotopomers.

V. Conclusions

The use of the low temperature, matrix-isolation technique provides narrow IR lines and spectra that are largely free of aggregate species compared with conventional sampling methods. It allows new assignments of the N–H In Plane Bending (NH-IPB) and N–H Out-of-Plane Bending (OPB) IR modes of free-base phthalocyanine. The assignments were confirmed by isotopic substitution with deuterium for the two central N–H bonds and by DFT calculations. The calculated frequencies are in very good agreement with the experimental values.

DFT calculations are an indispensable tool for band assignments and essential for predictions of non-observed vibrational modes. They are conducted on the three isotopomers of the free-base (H_2Pc , HDP, and D_2Pc) together with a metallo-phthalocyanine (ZnPc). An overview of the vibrations of these molecules is necessary to achieve global assignments and establish correlations between the modes of the four molecules. All the computational data, combined with IR and Raman experimental results, give a comprehensive overview of the vibrational behaviour of phthalocyanines, with a specific emphasis on the NH motion of the free-base molecule.

The NH stretching modes are confirmed to be well isolated from other motions of the Pc skeleton. Thus the NH(D) antisymmetric stretch of H_2Pc (D_2Pc) is located around 3310 (2480) cm^{-1} in rare gas matrices (a slightly higher value than in KBr) while the NH(D) stretch of HDPc is at 3337 (2500) cm^{-1} in the same solids. The H_2Pc (D_2Pc) symmetric stretch is predicted 52 (34) cm^{-1} above its antisymmetric counterpart, corresponding to very weak bands of Raman spectra in KBr located at 3343 cm^{-1} (2504 cm^{-1}).

Of the out-of-plane bending vibrations two modes, one of *gerade* symmetry the other *ungerade*, are clearly assigned to bands around 700 cm^{-1} for NH and around 500 cm^{-1} for ND. The symmetries of these modes are specified in Table 5 as B_{2g} and B_{1u} respectively. Only one of these two modes is IR active in H_2Pc and D_2Pc , specifically it is observed at 765 cm^{-1} and 555 cm^{-1} , respectively, in rare gas matrices. The corresponding NH band of HDPc has been experimentally identified at 742 cm^{-1} , whereas theoretical results clearly show a less isolated NH bending motion in this isotopomer. In partial agreement with Zhang's results,¹⁴ we find other OPB modes affected by H/D substitution.

Calculations established that previous assignments of the IR NH-IPB in H_2Pc and D_2Pc in KBr or Nujol were not correct. The present work leads only partly to the same conclusions as Zhang's calculations. The NH-IP bending modes are spread out over more than eight modes, four of which have been clearly identified in the matrix IR spectra. The others are predicted to be too weak to be observed. The IPB most affected modes by NH(D) motion are located between 750 and 1250 cm^{-1} for both IR and Raman modes. The largest observed $\nu_{\text{H}}/\nu_{\text{D}}$ ratio for this kind of mode is 1.085 for the band at 1045 cm^{-1} in the IR spectrum of H_2Pc in rare gas

matrices. The small ratio arises as a result of the strong coupling it has with other modes and its ensuing dilution over these modes.

Several N–H bending modes are predicted to exhibit the peculiar behaviour of having $\nu_{\text{H}} < \nu_{\text{D}}$ in H/D substitution work. Only one of these, an OPB mode, is observed in the infrared in the 730 cm^{-1} region. This behaviour can be traced back to the avoided-crossing of these modes by the “pure” N–H OP bending mode. This unusual effect has been examined in a theoretical study involving a continuous change of the isotopic mass from H_2Pc to D_2Pc . A consequence of this frequency increase in the heavier isotopomer is that the direction of the N–D OP bend is reversed from the N–H OP bending.

The spectral window between the C–H stretching and the N–H stretching modes (3100 – 3300 cm^{-1}) was carefully examined in the low temperature matrix-IR spectra for evidence of the *cis* isomer of H_2Pc , predicted by DFT calculations from the work of Strenalyuk *et al.*²⁷ to absorb in this region. One unaccounted band is located at 3104 cm^{-1} in Ar and using the scaling factor of 0.931 we found appropriate for the N–H stretch, it is close to the predicted value of 3094 cm^{-1} (unscaled 3323 cm^{-1}). However, as this band is only a partially resolved feature on the shoulder of the strongest C–H stretching mode of the dominant *trans* form, the existence of the unstable *cis* isomer cannot be identified in the present study. To examine this possibility adequately, one would propose working with $\text{H}_2\text{Pc}-d_{16}$ but in addition, a means of increasing the content of the *cis* form must be utilised. A possible approach for enhanced isolation of the *cis* form involves electronic promotion of the interconversion of the two *trans* forms of H_2Pc isolated at low temperatures.

The Raman spectra of H_2Pc in KBr reveal, as presented in Fig. 13, a striking resemblance with the fluorescence recorded by us for the same molecules isolated in rare gas and nitrogen

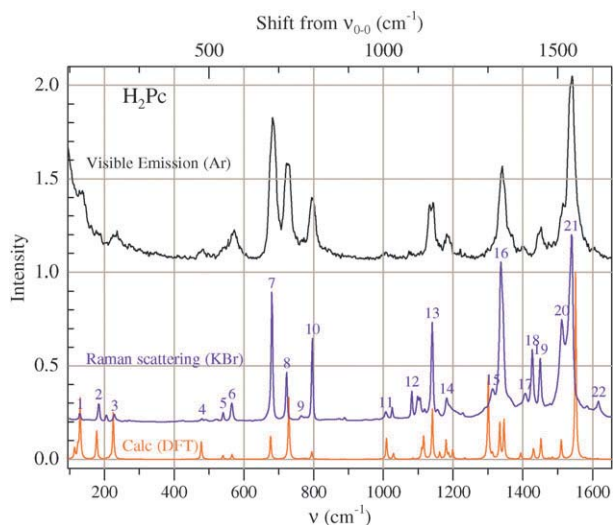


Fig. 13 A comparison of the experimentally recorded Raman spectrum and the visible fluorescence spectrum of H_2Pc in an Ar matrix. The correspondence between the two spectra is striking especially with regard to the line positions. DFT prediction of the ground state vibrations clearly allows assignment of the emission bands. The numbering provided shows the most intense modes in both Raman and emission whose motions have been determined in DFT calculations.

matrices.^{5,10} The very evident similarities between the recorded Raman scattering and the matrix fluorescence spectra indicate the close correspondence between the vibrational levels accessed in these transitions. This behaviour can be understood when it is noted that the observed Raman modes all involve in-plane vibrations and it is known^{9,34} that the fluorescence lines involve *gerade*, and in-plane vibrational modes of the ground state, more precisely A_{1g}, A_{2g}, B_{1g} and B_{2g} modes for ZnPc and A_g and B_{1g} modes for H₂Pc. Since the selection rules for Raman scattering and S₁-S₀ vibronic intensity distributions are very similar, the present Raman analysis will be very useful for band assignments of the emission spectra.

The ground state vibrational analysis conducted in this study is an essential precursor to understanding the transitions to and from the first excited electronic states. The Raman active N-H in-plane band observed at 1026.3 cm⁻¹ is identified as the most likely mode capable of coupling the $\nu = 0$ level of the S₂ (Q_Y) electronic state and vibrationally excited levels of the S₁ (Q_X) states of H₂Pc. Moreover, its shift to 986.1 cm⁻¹ for D₂Pc is fully consistent with Bondybey's results⁸ on fluorescence excitation of the H₂Pc and D₂Pc in solid Ar. The present results mark the beginning for a global analysis of the structure-frequency relationships of the Pcs with its parent molecule tetraazaporphine (TAP) and ultimately with the related family of porphine molecules. Currently no reliable, narrow line experimental data are known to exist for H₂TAP and while DFT predictions have been published,³⁵ no isotopic substitution results (either experimental or predicted) are available for the isotopomers HDTAP and D₂TAP. This deficiency will be addressed by us in the near future as we plan to record the matrix IR spectra of H₂TAP and perform DFT calculations of the isotopomers of this molecule.

Acknowledgements

This work was supported by the Science Foundation Ireland (SFI), Research Frontiers Programme (06/RFP/CHP012) Grant and an earlier SFI Basic Research (04/BR/C0182) grant. Travel support was provided by the Enterprise Ireland/CNRS "Ulysses" France-Ireland research exchange grant (2006). JMcC gratefully acknowledges a Professeur invitee position at the Universite Paris-Sud in March 2010 for the conclusion of this work.

References

- 1 F. M. Moser and A. L. Thomas, *Phthalocyanine Compounds*, Reinhold Publishing Corporation, New York, 1969.
- 2 T. Hanada, H. Takiguchi, Y. Okada, Y. Yoshida, N. Tanigaki and K. Yase, *J. Cryst. Growth*, 1999, **204**, 307.
- 3 J. L. Bredas, C. Adant, P. Tackx and A. Persoons, *Chem. Rev.*, 1994, **94**, 243.
- 4 S. G. Bown, C. J. Tralau, P. D. Coleridge Smith, D. Akdemir and T. J. Wieman, *Br. J. Cancer*, 1986, **54**, 43.
- 5 N. Dozova, C. Murray, J. G. McCaffrey, N. Shafizadeh and C. Crépin, *Phys. Chem. Chem. Phys.*, 2008, **10**, 2167.
- 6 P. S. H. Fitch, C. A. Haynam and D. H. Levy, *J. Chem. Phys.*, 1981, **74**, 6612.
- 7 R. Lehnig, M. Slipchenko, S. Kuma, T. Momose, B. Sartakov and A. Vilesov, *J. Chem. Phys.*, 2004, **121**, 9396.
- 8 V. E. Bondybey and J. H. English, *J. Am. Chem. Soc.*, 1979, **101**, 3446.
- 9 T.-H. Huang, K. E. Rieckhoff and E. M. Voigt, *J. Chem. Phys.*, 1982, **77**, 3424.
- 10 N. Dozova, C. Murray, J. G. McCaffrey, N. Shafizadeh and C. Crépin, manuscript in preparation, 2010.
- 11 H. F. Shurvell and L. Pinzuti, *Can. J. Chem.*, 1966, **44**, 2.
- 12 M. P. Sannes, *J. Chem. Soc., Perkin Trans. 2*, 1972, 160-162.
- 13 D. R. Tackley, G. Dent and W. E. Smith, *Phys. Chem. Chem. Phys.*, 2000, **3**, 3949.
- 14 X. Zhang, Y. Zhang and J. Jiang, *Vib. Spectrosc.*, 2003, **33**, 153-161.
- 15 D. R. Tackley, G. Dent and W. E. Smith, *Phys. Chem. Chem. Phys.*, 2001, **3**, 1419.
- 16 M. A. Collier and J. G. McCaffrey, *J. Chem. Phys.*, 2003, **119**, 11878.
- 17 P. S. H. Fitch, C. A. Hayman and D. H. Levy, *J. Chem. Phys.*, 1980, **73**, 1064.
- 18 M. J. Frisch, G. W. Trucks, H. B. Schlegel, G. E. Scuseria, M. A. Robb, J. R. Cheeseman, J. A. Montgomery, Jr., T. S. Dyden, K. N. Kudin, J. C. Burant, J. M. Millam, S. S. Iyengar, J. Tomasi, V. Barone, B. Mennucci, M. Cossi, G. Scalmani, N. Rega, G. A. Petersson, H. Nakatsuji, M. Hada, M. Ehara, K. Toyota, R. Fukuda, J. Hasegawa, M. Ishida, T. Nakajima, Y. Honda, O. Kitao, H. Nakai, M. Klene, X. Li, J. E. Knox, H. P. Hratchian, J. B. Cross, V. Bakken, C. Adamo, J. Jaramillo, R. Gomperts, R. E. Stratmann, O. Yazyev, A. J. Austin, R. Cammi, C. Pomelli, J. W. Ochterski, P. Y. Ayala, K. Morokuma, G. A. Voth, P. Salvador, J. J. Dannenberg, V. G. Zakrzewski, S. Dapprich, A. D. Daniels, M. C. Strain, O. Farkas, D. K. Malick, A. D. Rabuck, K. Raghavachari, J. B. Foresman, J. V. Ortiz, Q. Cui, A. G. Baboul, S. Clifford, J. Cioslowski, B. B. Stefanov, G. Liu, A. Liashenko, P. Piskorz, I. Komaromi, R. L. Martin, D. J. Fox, T. Keith, M. A. Al-Laham, C. Y. Peng, A. Nanayakkara, M. Challacombe, P. M. W. Gill, B. Johnson, W. Chen, M. W. Wong, C. Gonzalez and J. A. Pople, *Gaussian 03, Revision C.02*, Gaussian, Inc., Wallingford CT, 2004.
- 19 A. D. Becke, *Phys. Rev. A: At., Mol., Opt. Phys.*, 1988, **38**, 3098.
- 20 C. Lee, W. Yang and R. G. Parr, *Phys. Rev. B: Condens. Matter*, 1988, **37**, 785.
- 21 P. J. Stephens, F. J. Devlin, C. F. Chabalowski and M. J. Frisch, *J. Phys. Chem.*, 1994, **98**, 11623.
- 22 R. Ditchfield, W. J. Hehre and J. A. Pople, *J. Chem. Phys.*, 1971, **54**, 724.
- 23 N. Verdal, P. M. Kozłowski and B. S. Hudson, *J. Phys. Chem. A*, 2005, **109**, 5724.
- 24 D. Michalska and R. Wysokinski, *Chem. Phys. Lett.*, 2005, **403**, 211.
- 25 W. R. Scheidt and W. Dow, *J. Am. Chem. Soc.*, 1977, **99**, 1101.
- 26 K. A. Nguyen and R. Pachter, *J. Chem. Phys.*, 2001, **114**, 10757.
- 27 T. Strenalyuk, S. Samdal and H. Vidar-Volden, *J. Phys. Chem. A*, 2008, **112**, 4853.
- 28 The D_{2h} symmetry labels of the normal modes of H₂Pc produced by the Gaussian 03 package has, by convention, the z-axis aligned along the N-H bonds in the molecular plane. In contrast the z-axis is perpendicular to the plane of the molecule for the D_{4h} symmetry of ZnPc. For ease of comparison of the vibrational modes of these two molecules it is advantageous to re-orient the z-axis of H₂Pc perpendicular to the molecule plane. This has the effect of interchanging the 1 and 3 subscript labels of the Mulliken symbols.
- 29 L. L. Gladkov, V. K. Konstantinova, N. M. Ksenofontanova, N. A. Sokolov, K. N. Solov'ev and S. F. Shkirman, *J. Appl. Spectrosc.*, 2002, **69**, 47.
- 30 J. Liu, X. Zhang, Y. Zhang and J. Jiang, *Spectrochim. Acta, Part A*, 2007, **67**, 1232.
- 31 C. Murray, S. Fitzgerald and J. G. McCaffrey, unpublished results, 2009.
- 32 In examining the Raman isotope shifts, one must be mindful of the fact that the spectra were recorded for D₂Pc/KBr samples that contained residual amounts of H₂Pc. As a result, bands of H₂Pc sensitive to isotopic substitution decrease in intensity but are not completely removed.
- 33 S. F. Shkirman, N. A. Sokolov, V. K. Konstantinova and K. N. Solov'ev and, *J. Appl. Spectrosc.*, 2001, **68**, 410.
- 34 G. Herzberg, *Electronic Spectra of Polyatomic Molecules*, Litton Edition, van Nostrand Reinhold, N.Y., 1966.
- 35 D. Qi, Y. Zhang, X. Cai, J. Jiang and M. Bai, *J. Mol. Graphics Modell.*, 2009, **27**, 693.